Science of the Total Environment 907 (2024) 167832

Contents lists available at ScienceDirect

Science of the Total Environment

journal homepage: www.elsevier.com/locate/scitotenv

Metagenomic insights into the microbial cooperative networks of a benz(*a*)anthracene-7,12-dione degrading community from a creosote-contaminated soil

Sara N. Jiménez-Volkerink [a], Maria Jordán [a], Hauke Smidt [b], Cristina Minguillón [c], Joaquim Vila [a,*], Magdalena Grifoll [a]

[a] Department of Genetics, Microbiology and Statistics, University of Barcelona, Av. Diagonal, 643, 08028 Barcelona, Spain
[b] Laboratory of Microbiology, Wageningen University & Research, Stippeneng 4, 6708, WE, Wageningen, the Netherlands
[c] Department of Nutrition, Food Science and Gastronomy, University of Barcelona, Avda. Prat de la Riba, 171, 08921 Sta. Coloma de Gramanet, Barcelona, Spain

HIGHLIGHTS

- Different bacterial populations degrade the oxy-PAH B*a*AQ or its parent PAH, B*a*A.
- A B*a*AQ-degrading bacterial consortium was enriched in sand-in-liquid microcosms.
- Soil B*a*AQ metabolic network was rebuilt from metabolomic and metagenomic screens.
- Oxy-PAH degradation mechanisms are exchanged by horizontal gene transfer events.
- Nutritional interdependencies drive the microbial community assembly.

GRAPHICAL ABSTRACT

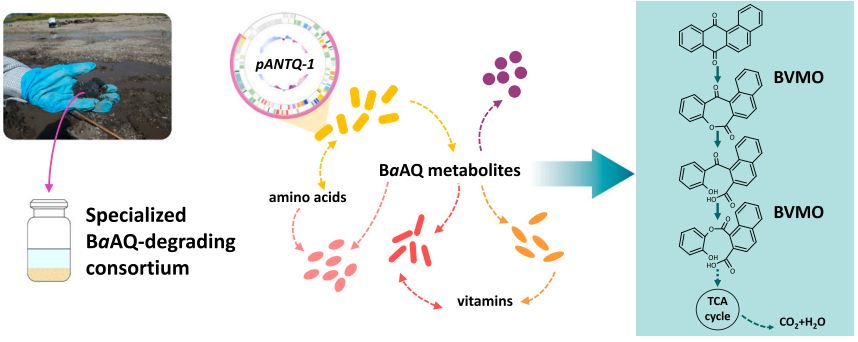

ARTICLE INFO

Editor: Jose Julio Ortega-Calvo

Keywords:
Oxy-PAHs
7,12-benz(*a*)anthraquinone
Bacterial consortium
Baeyer-Villiger
Horizontal gene transfer
Microbial interactions

ABSTRACT

Genotoxicity of PAH-contaminated soils can eventually increase after bioremediation due to the formation and accumulation of polar transformation products, mainly oxygenated PAHs (oxy-PAHs). Biodegradation of oxy-PAHs has been described in soils, but information on the microorganisms and mechanisms involved is still scarce. Benz(*a*)anthracene-7,12-dione (B*a*AQ), a transformation product from benz(*a*)anthracene frequently detected in soils, presents higher genotoxic potential than its parent PAH. Here, using sand-in-liquid microcosms we identified a specialized B*a*AQ-degrading subpopulation in a PAH-contaminated soil. A B*a*AQ-degrading microbial consortium was obtained by enrichment in sand-in-liquid cultures with B*a*AQ as sole carbon source, and its metagenomic analysis identified members of *Sphingobium*, *Stenotrophomonas*, *Pusillimonas*, *Olivibacter*, *Pseudomonas, Achromobacter,* and *Hyphomicrobiales* as major components. The integration of data from metabolomic and metagenomic functional gene analyses of the consortium revealed that the B*a*AQ metabolic pathway was initiated by Baeyer-Villiger monooxygenases (BVMOs). The presence of plasmid *pANTQ-1* in the metagenomic sequences, identified in a previous multi-omic characterization of a 9,10-anthraquinone-degrading isolate recovered from the same soil, suggested the occurrence of a horizontal gene transfer event. Further metagenomic

* Corresponding author.
E-mail address: qvila@ub.edu (J. Vila).

https://doi.org/10.1016/j.scitotenv.2023.167832
Received 31 July 2023; Received in revised form 11 October 2023; Accepted 12 October 2023
Available online 18 October 2023

analysis of the BaAQ-degrading consortium also provided insights into the potential roles and interactions within the consortium members. Several potential auxotrophies were detected, indicating that relevant nutritional interdependencies and syntrophic associations were taking place within the community members, not only to provide suitable carbon and energy sources, but also to supply essential nutrients and cofactors. Our work confirms the essential role that BVMO may play as a detoxification mechanism to mitigate the risk posed by oxy-PAH formation during bioremediation of contaminated soils.

1. Introduction

Oxygenated polycyclic aromatic hydrocarbons (oxy-PAHs) co-occur with PAHs in contaminated environments and are often regarded as more genotoxic, mutagenic and carcinogenic than their parent PAHs (Idowu et al., 2019). In addition, they are more water-soluble than unsubstituted PAHs, presenting higher environmental mobility and bioavailability (Larsson et al., 2018), thus increasing the risk for human and environmental health. Aromatic ketones and quinones are often produced as final products of branched metabolic pathways or by cometabolic reactions in bacteria (Grifoll et al., 1992; Moody et al., 2001; van Herwijnen et al., 2003), being specially relevant during the biodegradation of high molecular weight PAHs (Kanaly and Harayama, 2010). Formation and accumulation of oxy-PAHs has been associated with the eventual increase in genotoxicity after bioremediation of PAH-contaminated soils despite effective PAH removal (Chibwe et al., 2015; Tian et al., 2017). As a consequence, there is an increasing concern on the environmental fate of these polar transformation products.

Benz(*a*)anthracene-7,12-dione (B*a*AQ), the ready oxidation product of the 4-ring PAH benz(*a*)anthracene (B*a*A) commonly found in PAH-contaminated environments (Lundstedt et al., 2007), is of particular interest due to its demonstrated genotoxic and mutagenic properties (Clergé et al., 2019). In vivo assays using fish embryos have revealed that B*a*AQ presents higher genotoxic potential than its parent PAH or than the well-known carcinogen benzo(*a*)pyrene (Dasgupta et al., 2014; McCarrick et al., 2019). In soils, B*a*AQ can be formed by microbial transformation of B*a*A, but also as a result of photooxidation (Lehto et al., 2003) and chemical remediation treatments, such as Fenton oxidation (Lee and Hosomi, 2001) or ozonation (Yao et al., 1998). Several bacterial and fungal isolates have been reported to produce B*a*AQ from the transformation of B*a*A. Productive degradation of B*a*A by *Mycobacterium vanbaalenii* PYR-1 is initiated by dioxygenasic attack at the C-10,11 positions, however this PAH is simultaneously oxidized by lateral reactions at C-7,12 leading to the accumulation of B*a*AQ and subsequent ring cleavage products (Moody et al., 2005). Bacterial transformation of B*a*A to B*a*AQ has also been detected for a strain of *Paenibacillus* (Deka and Lahkar, 2017), and genomic and transcriptomic analysis of *Rhodococcus* sp. P14 revealed that partial oxidation of B*a*A to B*a*AQ could be attributed to the action of a cytochrome P450 monooxygenase (Luo et al., 2016). Ligninolytic fungi are also known to produce B*a*AQ from the oxidation of B*a*A, prompted by laccases or peroxidases (Cajthaml et al., 2006; Wu et al., 2010; Li et al., 2018). Removal of B*a*AQ has been observed after its transient accumulation during active PAH biodegradation in contaminated soils (Andersson et al., 2003; Lundstedt et al., 2003; Hu et al., 2014; Wilcke et al., 2014; Adrion et al., 2016), suggesting its possible reutilization by soil microbial communities. However, the microbial populations and mechanisms involved in its environmental fate are still unknown.

In this study, we demonstrate the existence of distinctive microbial populations driving the biodegradation of B*a*A or its ready oxidation product B*a*AQ in a creosote-contaminated soil using sand-in-liquid soil microcosms. Based on the identification of a specialized B*a*AQ-degrading microbial guild, we selected a B*a*AQ-degrading microbial consortium by enrichment cultures using this oxy-PAH as the sole carbon source. This consortium served as a model to investigate the metabolic networks involved in oxy-PAH biodegradation in PAH-contaminated soils. We determined the bacterial consortium dynamics during active B*a*AQ-degradation by transcriptomic quantification of relevant phylotypes, and by monitoring B*a*AQ removal together with metabolite formation. By integrating data from metabolomic screens and genome-resolved metagenomics, we ascertained the B*a*AQ metabolic pathway and revealed the metabolic capabilities and potential interactions between microbial community members.

2. Materials and methods

2.1. Chemicals

Benz(*a*)anthracene (B*a*A, 99 %) and benz(*a*)anthracene-7,12-dione (B*a*AQ, >97 %) were obtained from Sigma-Aldrich Chemie (Steinheim, Germany). Media and reagents were purchased from Panreac Química (Barcelona, Spain) or Merck (Darmstadt, Germany). Solvents (organic residue analysis grade) were obtained from J.T. Baker (Deventer, The Netherlands).

2.2. Soil

The creosote-polluted soil sample was originally collected from a historical wood-treating facility in southern Spain. This soil (silty clay loam-calcaric fulvisoil) presented a very high content in PACs, Σ17 PAHs = 25,791 ± 2112 mg·kg^{-1}, Σ7 oxy-PAHs =273 ± 9 mg·kg^{-1} and Σ7 N-PACs = 2568 ± 366 mg·kg^{-1}(Jiménez-Volkerink et al., 2023a).

2.3. BaA and BaAQ sand-in-liquid soil microcosms

Biodegradation of B*a*A and B*a*AQ by the microbial communities present in the creosote-contaminated soil was analyzed in small-scale sand-in-liquid microcosms. Microcosms consisted of sterile 20 mL-glass vials containing 6 mL mineral medium (Hareland et al., 1975) and 3 g of thin grain sea sand (Panreac, Barcelona, Spain) coated with 0.2 g·L^{-1} of either B*a*A (877 μM) or B*a*AQ (775 μM) added in acetone solution. Microcosms were inoculated with a sample of the creosote-contaminated soil preincubated for 21 days in aerobic conditions to minimize the concentration of native PAHs (Jiménez-Volkerink et al., 2023a). For each substrate, series of triplicate microcosms were incubated during 0, 3, 6, 10, 15, 20 and 25 days at 150 rpm and 25 °C. Identical triplicate but non-inoculated flasks were included as abiotic controls. At each incubation time, a set of triplicates was extracted for chemical analysis and another set of triplicates was used to obtain 1 mL samples containing sand and liquid for molecular analysis. Chemical extraction and analysis of residual B*a*A and B*a*AQ in the sand-in-liquid microcosms was performed as described in the Supplementary Material. Degradation rates were calculated dividing the difference in molar concentration between two time points by the difference in time between those time points in days. Nucleic acid extraction was performed using the procedures described in the Supplementary Material and submitted to 16S rRNA amplicon sequencing following cDNA synthesis.

2.4. 16S rRNA amplicon sequencing

Paired end reads (2x300bp) of the V1-V3 region of the 16S rRNA from triplicate cDNA samples of selected data points (0 and 20 days) from sand-in-liquid microcosm incubations were obtained using Illumina MiSeq equipment and reagents at Molecular Research DNA

(Shallowater, Texas, USA). Raw data was processed using mothur 1.45.3 following the MiSeq standard operating procedure (Kozich et al., 2013). The MiSeq libraries produced a total of 533,705 quality sequences with an average of 59,300 ± 3484 reads per sample. Sequences were aligned using SILVA v138 reference files (Quast et al., 2013) and clustered into operational taxonomic units (OTUs) with a distance criterion of 0.03. The OTU taxonomic affiliations were assigned to each representative sequence using the RDP (Ribosomal Database Project) database v9 (Cole et al., 2014). Rarefaction curves, library coverages and α-diversity indexes were estimated normalizing the number of reads/sample to that of the least represented sample (54,528 reads). Correspondence analysis (CA) was done using the *vegan* Community Ecology package v.2.5–7 (Oksanen et al., 2020) in R v.4.1.0.

2.5. Enrichment cultures to obtain the BaAQ-degrading bacterial consortium BQ

The B*a*AQ-degrading community from the creosote-contaminated soil was enriched using a sand-in-liquid culture system, as described elsewhere (Tauler et al., 2016). Briefly, the culture system consisted in 100-mL Erlenmeyer flasks containing mineral medium (20 mL) and washed sea sand (10 g) coated with B*a*AQ (0.2 $g{\cdot}L^{-1}$) as sole carbon source. The initial culture was inoculated with a 1 mL sample containing sand and liquid from the B*a*AQ-spiked sand-in-liquid soil microcosms incubated for 30 days. Every month, 0.7 mL of sand and liquid were transferred to a new flask. Incubation was conducted at 25 °C and 150 rpm. Routine denaturing gradient gel electrophoresis (DGGE) analyses were performed in the moment of the transfer to check the stability of the microbial community as described previously (Tauler et al., 2016). All experiments involving the B*a*AQ-degrading consortium BQ were inoculated with 30 day-cultures.

2.6. Time-course of BaAQ biodegradation by bacterial consortium BQ

Series of triplicate sand-in-liquid cultures (20 mL) with B*a*AQ as sole carbon source (0.2 $g{\cdot}L^{-1}$) were inoculated with 0.7 mL of consortium BQ and incubated during 0, 3, 5, 10, 15, 20, 25 and 30 days at 150 rpm and 25 °C. Identical uninoculated flasks were included as abiotic controls. At each incubation time, a set of triplicate cultures and controls were removed for chemical analysis. After filtration, the aqueous phase was extracted 5 times with 10 mL ethyl acetate in neutral conditions and 5 times in acidic conditions (pH 2.5). The solid phase was extracted 5 times in an ultrasonic bath with 20 mL dichloromethane/acetone (2:1, *v*/v). Extracts were analyzed by high pressure liquid chromatography (HPLC) as described in the Supplementary Material. Also, 1 mL samples were collected from an additional set of triplicate flasks and total DNA and RNA were extracted for molecular analysis. Extracts were used as template for qPCR amplifications to monitor the abundance (DNA) and activity/expression (RNA) of relevant phylotypes (16S rRNA) or functional genes (see below).

2.7. Identification of BaAQ metabolites

Metabolites accumulated during the degradation of B*a*AQ were identified in large-scale sand-in-liquid cultures of consortium BQ. Sand-in-liquid cultures were scaled up to 2000-mL Erlenmeyer flasks, containing 400 mL of mineral medium and 200 g of sand coated with B*a*AQ (0.2 $g{\cdot}L^{-1}$). Cultures were inoculated with 14 mL of consortium BQ and incubated for 10 and 20 days. Controls without cells were included to assess abiotic degradation. At each incubation time, the entire content of the flasks was filtrated (Whatman No.1), and the liquid phase was extracted with 5 × 100 mL ethyl acetate, then acidified to pH 2.5 (6 N HCl) and extracted again in the same manner. Neutral and acidic extracts were analyzed by HPLC and, further identification of detected metabolites was achieved by HPLC coupled to a high-resolution mass spectrometer using electrospray ionization in positive ionization mode (HPLC-ESI(+)-HRMS) and by gas chromatography coupled to mass spectrometry (GC–MS). Analytical details are described in the Supplementary Material.

2.8. 16S rRNA gene clone library of bacterial consortium BQ

Total DNA from consortium BQ after 18 transfers was used as template for PCR amplification using universal bacterial 16S rRNA gene-targeted primers 27F and 1492R (Weisburg et al., 1991) and the GoTaq Master Mix as described in the Supplementary Material. The PCR amplification product was visualized using 1 % agarose gel and cloned using the pGEM®-T Easy Vector cloning kit (Promega, Madison, USA). A total of 65 clones were randomly selected, and the corresponding plasmids were purified with the GenJET Plasmid Miniprep kit (Thermo Scientific, USA). All inserts were partially sequenced using universal primer 27F at Macrogen Europe (Madrid, Spain). Selected clones representing clusters of highly similar sequences (>99 %) were also sequenced with universal primer 1492R. The resulting DNA sequences were manually adjusted using BioEdit v.7.2.5 and analyzed using the *Classifier* and *Sequence Match* tools of the Ribosomal Database Project II (Maidak et al., 2001) and Blastn tool of GenBank.

2.9. Shotgun metagenomic sequencing and analysis

Total DNA extraction for shotgun metagenomic sequencing of consortium BQ was performed using DNeasy PowerSoil kit (QIAGEN, Germany) with some modifications. Four aliquots of 1.5 mL containing sand and liquid were obtained from a culture of consortium BQ incubated for 15 days. The four aliquots were centrifuged and the pellets containing the sand and bacterial cells were transferred to 4 independent bead tubes. 200 μL of phenol:chloroform:isoamylic (25:24:1) were added to each tube and bead beating was conducted for 45 s at 5500 rpm. Lysates were recovered by centrifugation and treated with 200 μL of chloroform: isoamylic (24:1) to remove residual phenol. The four tubes were processed independently until the final purification step, when DNA extracts from the 4 tubes were loaded on a single spin column. Total DNA was eluted in a final volume of 70 μL.

Metagenomic sequencing of the DNA from consortium BQ was performed using an Illumina PE150 NovaSeq 6000 platform at Novogene Europe Co. (Cambridge, UK). Quality filtering and removal of adapters, artifacts and Phix contamination was done on the received paired-end raw reads using BBduk tool from BBmap. Raw and trimmed read data quality was checked using FastQC (v0.11.8). Trimmed reads were assembled using metaSPAdes v3.11.1 (−meta option) with default parameters (Nurk et al., 2017). Assembly statistics was obtained with Quast v.5.1. The assembly was used for binning with the Metawrap v1.2 pipeline running the metaBAT2 and MaxBin2 algorithms, using trimmed reads for mapping and a minimum contig length of 1000 bp. Relative abundance of each bin was inferred by mapping reads to each bin with Bowtie2 v.2.4.2 (Langmead and Salzberg, 2012). Bin quality assessment was performed with CheckM v.1.0.18 (Parks et al., 2015) and bins were referred to as metagenome-assembled genomes (MAGs) when >90 % completeness and <5 % contamination was observed. Taxonomic classification of the MAGs was done using the Genome Taxonomy Database toolkit GTDB-Tk v.1.1.0 (Chaumeil et al., 2020). Functional annotation of the MAGs was performed using Prokka v.1.14.6 (Seemann, 2014). The GhostKOALA annotation server was used to reconstruct metabolic pathways.

2.10. Quantitative PCR analysis

The abundance of relevant phylotypes and genes from consortium BQ in sand-in-liquid samples was determined by quantitative PCR (qPCR) analysis. All qPCR reactions were carried out on an Applied Biosystems StepOnePlus Real-time PCR system using PowerUp Sybr Green Master Mix (Applied Biosystems, CA, USA), 1 μL of template and

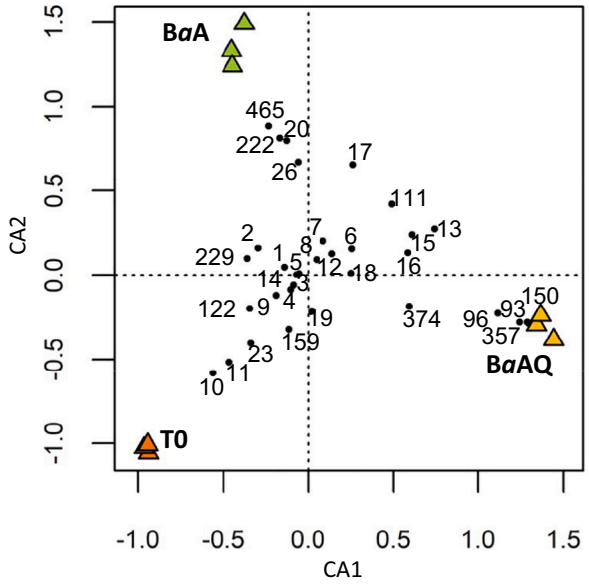

OTU	Taxonomic identification[a]	Class
1,3,5,374	*Sphingobium*	*α-proteobacteria*
7, 93, 465	Uncl. *Sphingomonadales*	
26,96, 150,222,357	Uncl. *Sphingomonadaceae*	
4	Uncl. *Rhodobacteraceae*	
6	*Caulobacter*	
12	Uncl. *Acetobacteraceae*	
14,16	Uncl. *Rhizobiaceae*	
15	*Bosea*	
17	Uncl. *Bradyrhizobiaceae*	
23	*Methylopila*	
8	*Achromobacter*	*β-proteobacteria*
2, 299	*Immundisolibacter*	*γ-proteobacteria*
9, 20, 122	Uncl. *Pseudomonadaceae*	
18, 19, 111, 159	*Pseudomonas*	
10	Uncl. *Xanthomonadaceae*	
13	Uncl. *Isosphaeraceae*	*Planctomycetacia*
11	Uncl. *Weeksellaceae*	*Flavobacteriia*

[a] When genus assignation had a probability lower than 100%, the immediate higher taxon with a 100% probability is shown.

Uncl. = unclassified

Fig. 1. Correspondence Analysis (CA) based on the relative contribution of the most active OTUs (>1%) in 16S rRNA transcript libraries from sand-in-liquid microcosms at 0 days (T0, orange triangles) and after 20 days of incubation with B*a*A (green triangles) or B*a*AQ (yellow triangles). Numbered black dots correspond to the distribution of OTUs. The first two axes (CA1 and CA2) of the CA explain 93.3% of the total variance observed. Table shows the taxonomic identification of the most active OTUs (>1%) in the sand-in-liquid soil microcosms, based on the RDP database.

4 pmol of each primer in a final volume of 20 μL. Total bacterial abundance (DNA) and activity (cDNA) were estimated by amplification of 16S rRNA genes and transcripts using universal primers 341F and 534R (Muyzer et al., 1993). Other than these, primers used for this study are listed in Table S1. Primers were designed using Primer-BLAST and experimentally validated by PCR. For quantification, six-point 10-fold standard dilution series were used. Amplification efficiency for all qPCR reactions ranged between 85 % and 110 % with a slope between −3.2 and − 3.8. Primer specificity was assessed by the observation of a single peak during melt curve analysis. Standards were prepared from the corresponding clone in the 16S rRNA clone library, or by cloning the gene amplicons using the pGEM-T Easy Vector System (Promega, WI, USA). Plasmids were purified with the GeneJET Plasmid Miniprep Kit (Thermo Scientific, USA), and validated by Sanger sequencing.

2.11. Data availability

Data from the 16S rRNA amplicon sequencing of sand-in-liquid microcosms and shotgun metagenomic sequencing of consortium BQ are deposited at NCBI under BioProject PRJNA932299. The Whole Genome Shotgun project is deposited at DDBJ/ENA/GenBank under the accession JAPRBE000000000. The metagenome-assembled genomes (MAGs) can be found under accession numbers JARYGI000000000 to JARYGW000000000. The 16S rRNA gene sequences from the clone library of consortium BQ can be found in GenBank under accession numbers OQ803208-OQ803220.

2.12. Statistical analysis

Data were subjected to analysis of variance (ANOVA) in IBM SPSS Statistics v.23 software, with mean differences significant at p-value <0.05.

3. Results and discussion

3.1. Bacterial populations driving the biodegradation of BaA and BaAQ in sand-in-liquid soil microcosms

Concentration of both B*a*A and B*a*AQ was significantly reduced in the respective sand-in-liquid soil microcosms after 25 days of incubation (B*a*A by 46 % and B*a*AQ by 55 %; Fig. S1). B*a*A biodegradation was initiated after a 3 days lag phase and continued until the end of incubation following first-order kinetics with an overall rate of 14.6 ± 0.8 $\mu mol \cdot L^{-1} \cdot day^{-1}$. B*a*AQ degradation started after an adaptation period of 6 days, and thereafter the oxy-PAH was also steadily consumed with first-order kinetics until the end of the incubation (12.4 ± 0.6 $\mu mol \cdot L^{-1} \cdot day^{-1}$). It is worth noting that the biodegradation of both compounds was still ongoing at the end of the experiment, suggesting that further removal could have been achieved with longer incubation times.

16S rRNA gene and transcript copy numbers were estimated by qPCR amplification as a proxy of bacterial abundance and activity, respectively. 16S rRNA gene copy numbers were relatively high at the beginning of the experiment ($1.3 \cdot 10^8 \pm 4 \cdot 10^7$ gene copies$\cdot mL^{-1}$), and only showed slight, but significant, increases after 10 days in microcosms with B*a*A ($3.6 \cdot 10^8 \pm 6.3 \cdot 10^7$ gene copies$\cdot mL^{-1}$) and after 6 days with B*a*AQ ($3.0 \cdot 10^8 \pm 3.5 \cdot 10^7$ gene copies$\cdot mL^{-1}$). 16S rRNA transcript copy numbers did not show any significant changes, with values ranging from $1.9 \cdot 10^{10} \pm 9.5 \cdot 10^9$ to $3.9 \cdot 10^{10} \pm 3.9 \cdot 10^9$ transcripts$\cdot mL^{-1}$ in all incubations. This high bacterial activity at the beginning of the experiment can be explained by the preincubation of the soil to reduce its PAHs content, while the fact that 16S rRNA gene transcripts remained two orders of magnitude higher than the 16S rRNA gene copies during the entire incubation indicates the presence of metabolically active populations.

Shifts in the active bacterial community structure were ascertained by 16S rRNA amplicon sequencing of cDNA samples from the sand-in-liquid soil microcosms. A predominance of *Alpha-* and *Gammaproteobacteria* was observed at the beginning of the experiment (47.2 and 47 % relative abundance, respectively) that persisted after 20 days of

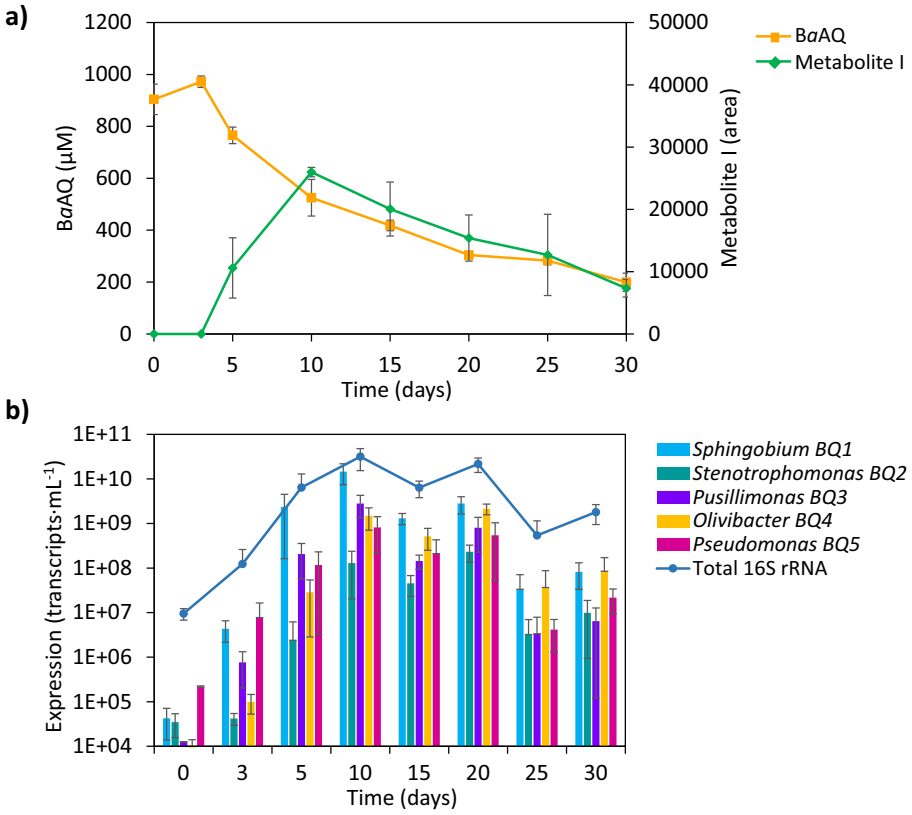

Fig. 2. (a) Evolution of B*a*AQ and metabolite I in sand-in-liquid cultures of consortium BQ. Abundance of metabolite I is represented as HPLC peak area. (b) Expression of representative phylotypes from consortium BQ and total 16S rRNA transcripts·mL^{-1} along incubation with B*a*AQ as sole carbon source in sand-in-liquid cultures. Values are average of three independent cultures and error bars represent standard deviation.

incubation with B*a*A (54.1 % and 36.8 %) or B*a*AQ (65.6 % and 23.1 %). However, relevant changes were detected in the relative expression of certain OTUs (Fig. S2), and correspondence analysis of the most relatively active OTUs (>1 %) highlighted the clear divergence in the microbial community profiles associated with either B*a*A or B*a*AQ degradation (Fig. 1). In the B*a*A-spiked microcosms, OTU 2 affiliated to the genus *Immundisolibacter* (Corteselli et al., 2017) was the most active OTU, showing a significant increase in relative abundance in cDNA derived sequences compared to time 0 (from 11.5 % to 13.7 %). In fact, the 16S rRNA gene sequence of OTU 2 shared a 100 % identity to that of the *Immundisolibacter* phylotype identified as the key player in the biodegradation of B*a*A applying DNA stable isotope probing (SIP) in a previous study using soil from the same site (Jiménez-Volkerink et al., 2023b). Other less abundant OTUs that significantly incremented in the B*a*A-microcosms were unclassified *Pseudomonadaceae* (OTU 20, from 0.4 % to 2.7 %) and several sphingomonads (OTU 465, from 0.16 % to 1.1 %; OTU 26, from 0.19 % to 0.98 %; OTU 222, from 0.14 % to 0.94 %). Conversely, in the presence of B*a*AQ there was a dramatic increase in the relative abundance of an unclassified member of *Sphingomonadales* (OTU 93, from 0.28 % to 12.3 %), becoming the most relatively active phylotype in the community. Less pronounced increases were observed for other members of this order (OTU 150, from 0.04 % to 1.9 %; OTU 96, from 0.12 % to 1.8 %; OTU 357, from 0.06 % to 1.6 %; OTU 374, from 0.28 to 0.85 %), suggesting that B*a*AQ might be degraded by a specialized uncultured group of *Sphingomonadales*. We have recently isolated a strain of *Sphingobium* sp., AntQ-1 (Jiménez-Volkerink et al., 2023a) specialized in the degradation of 9,10-anthraquinone, a ready oxidation product from anthracene analogous to B*a*AQ. Altogether, these findings enlarge the broad catabolic range of sphingomonads (Aylward et al., 2013), and reinforce their role in the utilization of oxy-PAHs.

The above results confirm the existence of bacterial populations specialized in the biodegradation of polar PAH transformation products, as none of the B*a*AQ-associated phylotypes were significantly expressed in B*a*A-spiked microcosms. An analogous experiment using sand-in-liquid soil microcosms from the same soil spiked with either anthracene or anthraquinone revealed a similar divergence, indicating the existence of oxy-PAH-degrading specialists (Jiménez-Volkerink et al., 2023a). Rodgers-Vieira et al. (2015) applied DNA-SIP to a different PAH-contaminated soil and demonstrated that anthracene and anthraquinone were assimilated by different bacterial populations. Thus, it becomes highly likely that microbial communities from PAH-contaminated soils harbor populations with interconnected metabolic pathways, where dead-end products formed by certain microbial populations become substrates for others.

3.2. *BaAQ-degrading bacterial consortium BQ*

Using the B*a*AQ-spiked sand-in-liquid soil microcosms as inoculum, a B*a*AQ-degrading bacterial consortium was established by sequential enrichment in sand-in-liquid cultures with B*a*AQ as sole carbon source. Consortium BQ has been maintained by monthly transfers for 1.5 years, and routine 16S rRNA gene PCR-DGGE analysis has shown a highly stable bacterial community structure (Fig. S3). Cultures of consortium BQ removed 80 % of the initial B*a*AQ concentration in 30 days. Strikingly, consortium BQ was not able to attack B*a*A, the parent PAH of B*a*AQ, reinforcing its high degree of specialization.

16S rRNA gene clone library analysis revealed that consortium BQ comprised 13 bacterial phylotypes (Table S2). The microbial community was dominated by a member of *Sphingobium* (BQ1, 32.5 %), the 16S rRNA gene sequence of which shared 98.2 % identity with that of OTUs 93 and 96 associated with the utilization of B*a*AQ in the sand-in-liquid

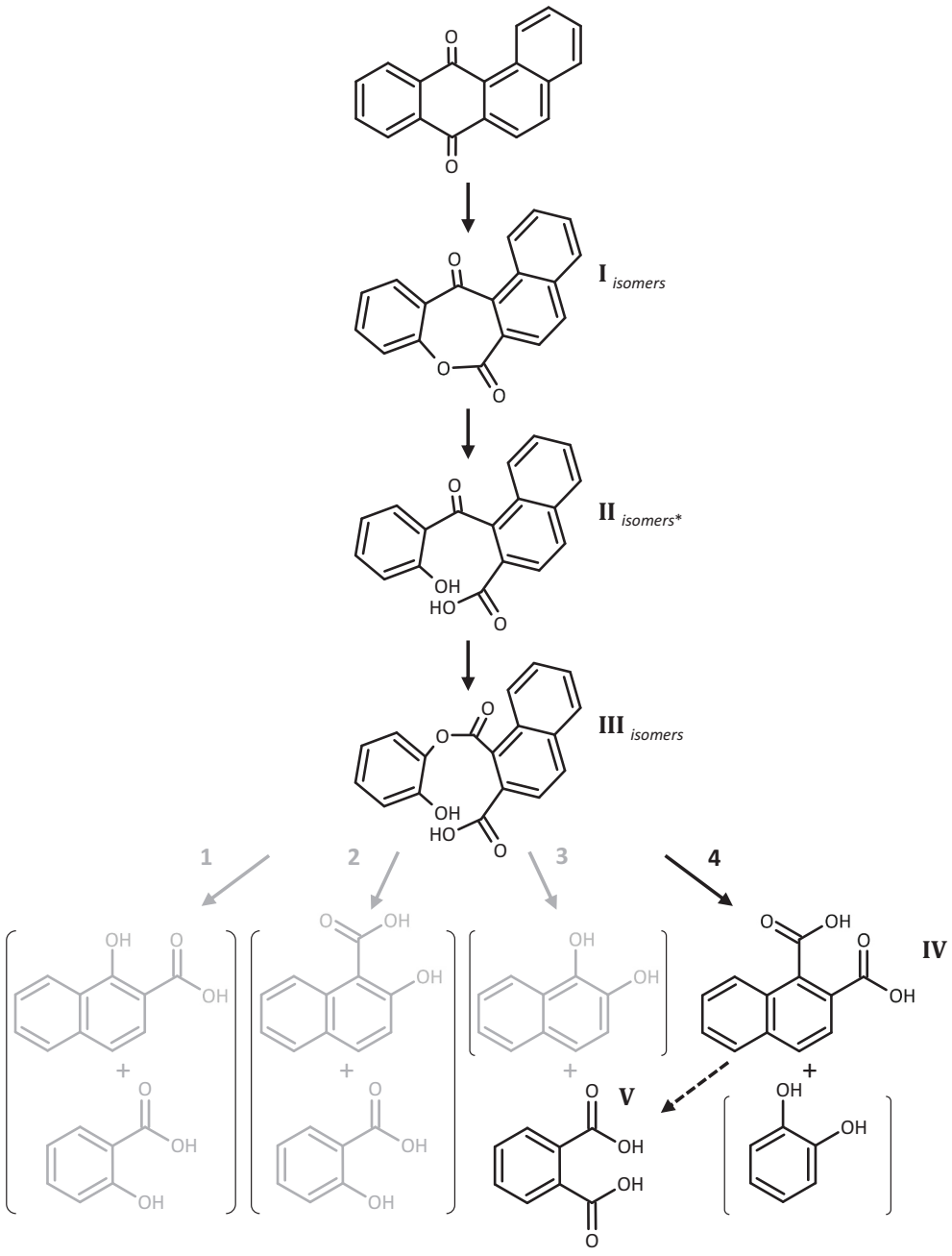

Fig. 3. Schematic pathway proposed for the degradation of benz(*a*)anthracene-7,12-dione by bacterial consortium BQ. Only one of the possible isomers of metabolites I, II and III is represented. Compounds in brackets were not detected. Numbered steps correspond to the possible metabolites resulting from the second Baeyer-Villiger reaction. (1) 1-hydroxy-2-naphthoic acid and salicylic acid, (2) 2-hydroxy-1-naphthoic acid and salicylic acid, (3) 1,2-dihydroxynapthtalene and phthalic acid, or (4) naphthalene dicarboxylic acid and catechol. Pathway in black is considered the predominant one. * Four isomers were detected for metabolite II: 1-(2-hydroxybenzoyl)naphthalene-2-carboxylic acid, 2-(2-hydroxynaphthalene-1-carbonyl)benzoic acid, 2-(1-hydroxynaphthalene-2-carbonyl)benzoic acid and 2-(2-hydroxybenzoyl)naphthalene-1-carboxylic acid.

soil microcosms. Interestingly, phylotype BQ1 was closely related (99 % identity) to an uncultured *Sphingobium* clone from a DNA-SIP experiment with [U-^{13}C]-anthracene that increased in abundance after the added anthracene had been consumed, suggesting the possible growth on anthracene metabolites (Jones et al., 2011). Other abundant members of consortium BQ were related to *Stenotrophomonas* (BQ2, 23.7 %; BQ6, 2.6 %), *Pusillimonas* (BQ3, 12.3 %; BQ9, 1.8 %), *Olivibacter* (BQ4, 8.8 %) and *Pseudomonas* (BQ5, 7.0 %). Sequences of *Stenotrophomonas* BQ2 were very similar (>99 %) to 16S rRNA sequences retrieved from other PAH/oil-contaminated soils (Accession numbers: HQ218574, KY962735), but also from plant rhizospheres (HQ912766, FJ493060, KT825842). *Pusillimonas* BQ3 and BQ9 were closely related to isolates of this genus with the ability to utilize hydroxybenzoates (NR_146844), substituted salicylates (NR_043129) or 5-hydroxypicolinic acid (KC602498), suggesting their role in the metabolism of aromatic acids. As for *Olivibacter* BQ4, its sequence resembled (99 %) that of an *Olivibacter* sp. strain UBH15, previously isolated from soil from the same site than the soil used here (Tauler et al., 2016). This strain was not able to remove any PAH from a creosote HMW-PAH residue, however, growth was observed at the expense of diphenic acid, protocatechuic acid, phthalic acid, 9-fluorenone-4-carboxylic acid and 1,2,3-benzenetricarboxylic acid (data not shown). The 16S rRNA gene of *Pseudomonas*

BQ5 showed high identity (>99 %) to isolates from PAH-contaminated soils and sediments (MT448942; MF928390), isolates with the ability to degrade xenobiotics such as diethyl phthalate (MN964893) or pymetrozine (MW674665), and to the well-characterized *P. putida* KT2440, which is known for its wide metabolic versatility towards aromatic compounds (Belda et al., 2016). Less abundant constituents of consortium BQ were affiliated to *Achromobacter* (BQ8, 2.6 %), *Sphingomonadaceae* (BQ7, 2.6 %; BQ10, 1.8 %) and members of the *Hyphomicrobiales* order including *Bosea* (BQ11, 1.8 %), *Rhizobium* (BQ12, 1.8 %) and *Bradyrhizobium* (BQ13, 0.9 %).

3.3. Bacterial community dynamics during active BaAQ-biodegradation by consortium BQ

Insight into the bacterial community dynamics of consortium BQ was accomplished by quantifying the expression of selected phylotypes in the course of B*a*AQ removal (Fig. 2). After a 3-day lag phase, B*a*AQ was depleted following first-order kinetics with maximum biodegradation rates until the 10th day of incubation (54.2 ± 10.1 μmol·L^{-1}·day^{-1}), that attenuated thereafter. Coinciding with maximum B*a*AQ degradation rates, there was a maximum of accumulation of metabolite I. Afterwards it progressively decreased, indicating its subsequent uptake by the consortium members.

In the course of the incubation, we quantified the expression level of the most abundant phylotypes in the consortium, *Sphingobium* BQ1, *Stenotrophomonas* BQ2, *Pusillimonas* BQ3, *Olivibacter* BQ4 and *Pseudomonas* BQ5, by qPCR amplification specifically targeting their 16S rRNA transcripts. Bacterial activity, estimated as total 16S rRNA transcripts, experienced a significant increase after 3 days and reached its maximum at 10 days, coinciding with the highest B*a*AQ degradation rates. During this period, *Sphingobium* BQ1 was the most active phylotype in the consortium, with specific 16S rRNA transcripts 1 to 3 orders of magnitude above the rest, and reaching its maximum at 10 days of incubation ($1.1{\cdot}10^{10} \pm 7.2{\cdot}10^{9}$ transcripts·mL^{-1}). This peak of activity of phylotype BQ1 was concomitant with a maximum in the concentration of one of the metabolites detected in the culture fluids (metabolite I, see below), suggesting that this phylotype could be the main player in the initial attack of B*a*AQ. *Pusillimonas* BQ3 and *Pseudomonas* BQ5 showed their maximum expression in the same incubation period (10^{7} to 10^{9} transcripts·mL^{-1}). *Stenotrophomonas* BQ2 and *Olivibacter* BQ4, on the contrary, reached their maximum of expression at 20 days (10^{8} to 10^{9} transcripts·mL^{-1}) when B*a*AQ degradation was significantly attenuated. These results suggest that phylotypes BQ2 and BQ4 were likely feeding on transformation products produced by other members of consortium BQ. The simultaneous expression of different phylotypes within the community suggests that interactions are taking place during active biodegradation of B*a*AQ.

3.4. Identification of benz(a)anthracene-7,12-dione metabolites

Metabolites from the biodegradation of B*a*AQ by consortium BQ were identified by HPLC-ESI(+)-HRMS and GC–MS analyses of neutral and acidic culture extracts (Table S3). Tentative identification of metabolites was based on their exact mass and MS fragmentation patterns. Metabolite I was only detected in HPLC-ESI(+)-HRMS analyses and it produced the molecular formula $C_{18}H_{11}O_3$ ($[M + H]^+ = 275.0684$), showing ion fragments at *m/z* 275.0684 (100) and 247.0727 (3). The UV–visible spectrum presented λ_{max} at 220, 245, 335 and 370 nm. The exact mass is compatible with both a hydroxybenz(*a*)anthracene-7,12-dione and with an aromatic lactone resulting from a Bayer-Villiger monooxygenation at one of the possible positions of B*a*AQ (i.e. benzo(*b*)naphtho(1,2-*e*)oxepine-7,13-dione or a structural isomer). However, the further detection of a group of structural isomers (metabolites $II_{a\text{-}d}$) identified as the products of the hydrolysis of the four possible lactones indicated that metabolite I most probably corresponded to an isomeric form of the lactone benzo(*b*)naphtho(1,2-*e*)oxepine-7,13-dione. In HPLC-ESI(+)-HRMS, metabolites II were detected as two peaks with identical spectral characteristics: $[M + H]^+ = 293.0809$, corresponding to a molecular formula $C_{18}H_{13}O_4$, with ion fragments at *m/z* 293.0809 (64), 275.0704 (57), 249.0911 (100), 231.0807 (75), 219.0802 (11), 202.0773 (14), 189.0666 (11) and 165.0689 (9), and a UV/vis spectrum with λ_{max} at 230 and 294 nm. GC–MS analysis of the derivatized neutral extract resolved the four possible isomers, detected as four peaks with identical fragmentation pattern and with major fragment ions at *m/z* 306 (M+, 32), 274 (100), 246 (91), 218 (32), 189 (38), 163 (15), 115 (38) and 77 (21). According with these spectral characteristics these metabolites were identified as the methyl ester derivatives of 1-(2-hydroxybenzoyl)-2-naphthoic acid, 2-(2-hydroxynaphthalene-1-carbonyl)benzoic acid, 2-(2-hydroxybenzoyl)naphthalene-1-carboxylic acid and or 2-(1-hydroxynaphthalene-2-carbonyl)benzoic acid, four isomers that differ on the position of the carboxyl and hydroxyl groups. The detection of four isomers indicates that the Baeyer-Villiger (BV) oxidation and further hydrolysis occur at the four possible positions, nevertheless one of the isomers clearly predominated over the others, indicating a preferential route for lactone production (see below).

The identification of the benzo(*b*)naphtho(1,2-*e*)oxepine-7,13-dione isomer (metabolite I) and the four isomers of 1-(2-hydroxybenzoyl)-2-naphthoic acid (metabolites $II_{a\text{-}d}$) as major metabolites from B*a*AQ suggests that consortium BQ first attacks the quinone ring and further metabolizes the aromatic rings to intermediates of the central metabolism (Fig. 3). The attack would be initiated by a biological BV oxidation producing a lactone that would eventually be hydrolyzed resulting in the ring cleavage of the quinone ring. A similar mechanism has been recently described for the degradation of 9,10-anthraquinone (ANTQ) by *Sphingobium* sp. AntQ-1 (Jiménez-Volkerink et al., 2023a). In that strain, ANTQ degradation was suggested to proceed through two successive BV oxidations, based on the overexpression of two gene clusters coding for BV monooxygenases (BVMO) together with associated hydrolases, and of the genes coding for both phthalate and catechol metabolic pathways. Here, HPLC-ESI(+)-HRMS analysis of the acidic extracts from consortium BQ cultures revealed a product (metabolite III) with an exact mass of $[M + H]^+ = 309.0756$, corresponding to the molecular formula $C_{18}H_{13}O_5$, with ion fragments at *m/z* 309.0756 (59), 291.0652 (100) and 215.0335 (30). These properties are compatible with an isomeric form of 1-[(2-hydroxyphenoxy)carbonyl]naphthalene-2-carboxylic acid, which would also suggest that consortium BQ performs a second BV attack on the detected acids (metabolites $II_{a\text{-}d}$).

Depending on the position of the carboxyl and hydroxyl moieties in metabolites II and III, four sets of subsequent metabolites may be formed: i) 1-hydroxy-2-naphthoic acid and salicylic acid, ii) 2-hydroxy-1-naphthoic acid and salicylic acid, iii) 1,2-dihydroxynapthtalene and phthalic acid, or iv) naphthalene-1,2-dicarboxylic acid and catechol (Fig. 3). However, only 1,2-naphthalenedicarboxylic acid (metabolite IV) and phthalic acid (metabolite V) were detected in culture extracts. Metabolite IV was identified as 1,2-naphthalenedicarboxylic acid based on its spectral characteristics. In HPLC-ESI(+)-HRMS it produced an exact mass of $[M + H]^+ = 217.0495$, corresponding to the formula $C_{12}H_9O_4$, with ion fragments at *m/z* 217.0495 (27) and 199.0390 (100). In GC–MS analyses of derivatized acidic extracts, the fragmentation spectrum matched with a dimethyl ester derivative of a naphthalenedicarboxylic acid, given that this product resulted from the oxidation of B*a*AQ, metabolite IV was identified as 1,2-naphthalenedicarboxylic acid. Metabolite V was identified as the dimethyl ester derivative of phthalic acid in GC–MS analysis of diazomethane-treated extracts. Identification was established on the basis of its MS spectrum (Table S3) and by comparison with authentic material.

The identification of 1,2-naphthalenedicarboxylic acid and phthalic acid could be indicative of B*a*AQ biodegradation being preferentially channeled to the formation of either 1,2-naphthalenedicarboxylic acid and catechol, or 1,2-dihydroxynapthtalene and phthalic acid. However, phthalic acid could also be produced from the further degradation of 1,2-napthtalenedicarboxilyc acid. These observations are in agreement

Table 1
Features of the metagenome assembled genomes (MAG) recovered from shotgun metagenomic sequencing of consortium BQ.

MAG	GTDB classification[a]	Size (Mbp)	GC (%)	Comp[b] (%)	Cont[b] (%)	Rel.[c] abun. (%)	Phylotype[d]	Freq. in clone library (%)
1	*Sphingobium*	3.86	62.0	99.1	0.69	31.0	*Sphingobium* BQ1	32.5
2	*Stenotrophomonas*	3.95	66.4	99.5	2.63	19.6	*Stenotrophomonas* BQ2	23.7
3	*Pusillimonas*	3.67	63.2	96.7	0.00	10.5	*Pusillimonas* BQ3	12.3
4	*Pseudosphingobacterium*	6.72	41.1	100	0.95	8.9	*Olivibacter* BQ4	8.8
5	*Pigmentiphaga*	4.46	65.3	87.8	0.61	3.5	*Pusillimonas* BQ9	1.8
6	*Stenotrophomonas*	4.04	67.2	74.1	0.00	3.2	*Stenotrophomonas* BQ6	2.6
7	*Sphingobium*	3.24	65.8	97.5	0.26	2.2	*Sphingobium* BQ7	2.6
8	*Sphingomonas*	3.76	67.5	97.6	0.00	2.1	*Sphingomonadaceae* BQ10	1.8
9	*Shinella*	6.83	63.8	98.7	0.39	1.6	*Rhizobium* BQ12[e]	1.8
10	*Bradyrhizobium*	8.02	64.0	99.4	1.35	1.5	*Bradyrhizobium* BQ13	0.9
11	*Achromobacter*	6.25	67.6	90.9	0.86	1.2	*Achromobacter* BQ8[e]	2.6
12	*Achromobacter*	6.18	64.8	91.3	1.79	1.1	*Achromobacter* BQ8[e]	2.6
13	*Rhizobiaceae*	6.37	62.2	97.9	2.28	1.1	*Rhizobium* BQ12[e]	1.8
14	*Pseudomonas*	5.33	61.8	96.7	1.15	0.6	*Pseudomonas* BQ5	7.0
15	*Bosea*	5.78	65.4	89.4	2.35	0.5	*Bosea* BQ11	1.8

[a] Taxonomic identification was based on the GTDB-Tk tool.
[b] Genome completeness and contamination were calculated with CheckM v.1.0.18.
[c] Relative abundance was inferred by mapping paired-end reads to each bin with Bowtie2.
[d] MAGs were assigned to each phylotype according to their taxonomic affiliation and their relative abundance in consortium BQ.
[e] These phylotypes were assigned to two different MAGs.

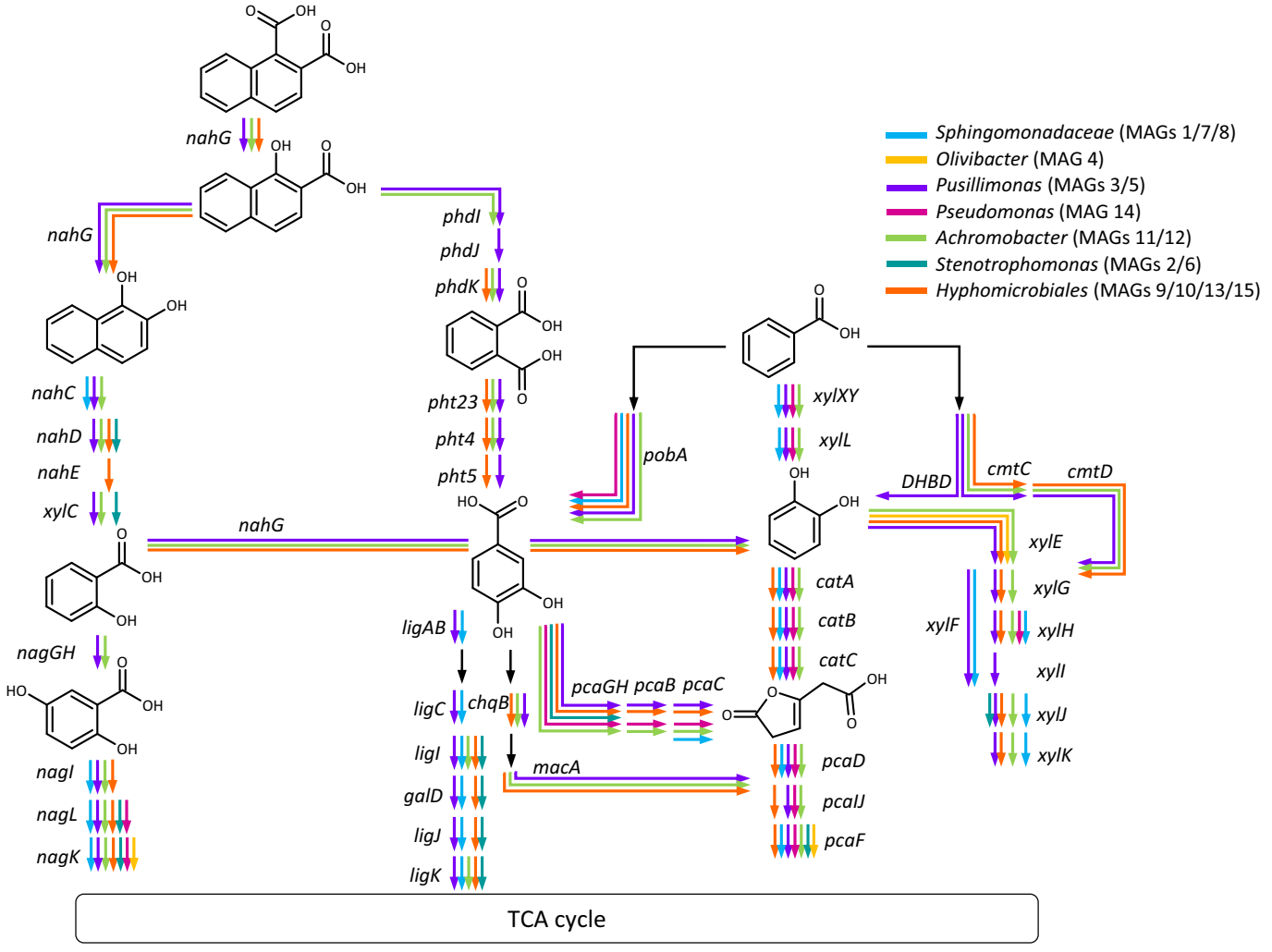

Fig. 4. Potential metabolic routes involved in the further degradation of the identified and hypothesized intermediates resulting from the upper BaAQ degradation pathway (Fig. 3). Reactions have been inferred from the annotated genes in the MAGs from consortium BQ. MAGs were grouped according to their taxonomic identification. Arrows labeled as different colors indicate genes found in each group of MAGs belonging to the same taxon.

with the previously described pathway for the degradation of anthraquinone by the ANTQ-degrading *Sphingobium* sp. strain AntQ-1, where both BV oxidations were performed symmetrically, producing phthalic acid and catechol. On this basis it seems that the predominant pathway for B*a*AQ biodegradation would proceed via production of 1,2-naphthalenedicarboxylic acid and catechol.

In summary, the most robust pathway for the biodegradation of B*a*AQ by consortium BQ would be initiated with a BV oxidation at the C-7 ketonic group, in which a new oxigen atom is introduced between the C-7 and the phenyl group producing the lactone benzo(*b*)naphtho(1,2-*e*) oxepine-7,13-dione. This lactone would then be hydrolyzed to produce 1-(2-hydroxybenzoyl)-2-naphthoic acid (Fig. 3). Subsequently, a second BV oxidation would occur at the C-13 ketonic group of this acid, producing 1-[(2-hydroxyphenoxy)carbonyl]naphthalene-2-carboxylic acid, and its hydrolyzation would lead to the formation of 1,2-naphthalenedicarboxylic acid and catechol. The formation of 1-(2-hydroxybenzoyl)-2-naphthoic acid from B*a*AQ was also reported for the transformation of B*a*A via B*a*AQ by *Mycobacterium vanbaalenii* PYR-1 (Moody et al., 2005), however, it was not attributed to a BV reaction.

3.5. Metabolic functional analysis of bacterial consortium BQ by shotgun metagenomics

Metabolic capabilities and potential interactions within members of consortium BQ were assessed by functional analysis of metagenome assembled genomes (MAGs). Shotgun metagenomic sequencing of DNA from a 15-days culture of consortium BQ generated a total of 36.8 million quality-filtered 150 bp paired-end reads that were assembled into 71,695 contigs (largest contig 926,254 bp, N50 64,905 bp) and binned into 15 high-quality MAGs (Table 1). The MAGs accounted for an 88.7 % of the total reads. Despite no 16S rRNA gene sequences were binned into any of the MAGs, most of the MAGs could be assigned to BQ phylotypes based on their phylogenomic affiliation, and comparison of their relative abundance in the metagenomic assembly and 16S rRNA gene clone library. Functional annotation of individual MAGs revealed the presence of genes predicted to encode for enzymes involved in the metabolism of aromatic compounds in all MAGs (Table S4).

As discussed above, B*a*AQ degradation would be initiated by the action of a BV monooxygenase. BVMOs are considered flavin-dependent monooxygenases (FDMOs) that catalyze BV oxidations (Tolmie et al., 2019). Depending on the type of flavin cofactor, the type of electron donor, the type of reaction catalyzed and the protein folding, FDMOs are classified into eight classes (van Berkel et al., 2006). Only classes A, B and C are known to include BVMOs. Table S5 summarizes the putative FDMOs belonging to these three classes detected in consortium BQ metagenome. Class A FDMOs encompass a diverse group of atypical BVMOs (type O) that are mostly multifunctional enzymes catalyzing enzyme cascades that include hydroxylation reactions in addition to the BV oxidation. Class B includes the most extensively studied BVMOs, which are type I. Scanning MAGs for the type I signature protein motif (Fraaije et al., 2002) revealed the presence of type I BVMOs in the MAGs of *Pseudomonas* BQ5 (MAG14_0903, MAG14_0921, MAG14_4357), *Bosea* BQ11 (MAG15_2077) and *Bradyrhizobium* BQ13 (MAG10_0840, MAG10_3680, MAG10_5155, MAG10_7237). The BVMO of *Sphingobium* sp. AntQ-1 involved in the second BV reaction in the metabolism of ANTQ is a type I BVMO (sphantq_4479), thus, the detected BVMOs might be driving the analogous step in the B*a*AQ metabolic pathway. The most closely related type I BVMOs to sphantq_4479 were the three coding sequences (CDS) of *Pseudomonas* BQ5 (48.2–48.8 % amino acid sequence identity, Fig. S4).

On the other hand, the BVMO catalyzing the initial attack of ANTQ by *Sphingobium* sp. AntQ-1 (sphantq_4473) was identified as a probable type II BVMO, that belong to class C FDMOs. To date, the only representatives of type II BVMOs are two diketocamphane monooxygenases (Iwaki et al., 2013). The MAGs of *Sphingobium* BQ1 (MAG1_2582), *Achromobacter* (MAG11_3219), *Bradyrhizobium* BQ13 (MAG10_5918) and *Rhizobium* (MAG13_5954) enclosed genes coding for diketocamphane monooxygenases, however, phylogenetic analysis of amino acid sequences revealed they were distantly related to sphantq_4473. In fact, sphantq_4473 closest relative was a CDS of *Pusillimonas* BQ9 (MAG5_4095) annotated as an alkanal monooxygenase, only sharing a 34.7 % identity (Fig. S4). Nevertheless, ANTQ-BVMOs of strain AntQ-1 were both part of a cluster composed by two genes, one coding for BVMO and the other for a hydrolase that would catalyze the hydrolyzation of the lactone. From all the potential BVMOs enclosed in the MAGs, only the three type I BVMOs of *Pseudomonas* BQ5 and a type II BVMO of *Pusillimonas* BQ9 (MAG5_3989) were accompanied by a hydrolase-coding gene.

Comprehensive reconstruction of the metabolic pathways enclosed in the MAGs revealed the metabolic potential of each phylotype to further process the downstream aromatic intermediates produced from B*a*AQ degradation (Fig. 4, Table S6). As argued before, the predominant pathway would lead to catechol and 1,2-naphthalenedicarboxylic acid. Previous studies with the phenanthrene-degrading strain *Arthrobacter* sp. P1–1 demonstrated that the latter can be further channeled to the central metabolism following two consecutive substitution reactions (from carboxyl to hydroxyl group) leading to the formation of 2-hydroxy-1-naphthoic and 1,2-dihydroxynaphthalene, respectively (Seo et al., 2006; Mallick et al., 2011). These substitution reactions can be probably attributed to the action of a salicylate hydroxylase, encoded by the gene *nahG*. Enzymatic assays with the salicylate hydroxylase from the phenanthrene-degrading strain *Pseudomonas putida* BS202-P1 catalyzed the conversion of 2-hydroxy-1-naphthoic to 1,2-dihydroxynaphthalene (Balashova et al., 2001). Surprisingly, the most abundant phylotype in consortium BQ, *Sphingobium* BQ1 (MAG1), did not harbor any complete pathway for aromatic compound processing. It only presented a *nahC* gene encoding for a 1,2-dihydroxynaphthalene dioxygenase, genes encoding for a benzoate 1,2-dioxygenase (*xylXYZ*), and some scattered genes coding for intermediate or final steps in the catechol or gentisate pathways, respectively (*xylF* and *nagLK*). The less abundant *Sphingobium* BQ7 (MAG7) possessed the complete protocatechuate *meta*-cleavage pathway (*ligABCIJK* and *galD*) and *Sphingomonadaceae* BQ10 (MAG8) had genes coding for the initial steps for catechol *ortho*-cleavage (*catABC* and *pcaD*). However, the metabolic potential of these phylotypes might be underestimated as it is widely known that sphingomonads often harbor aromatic degradative genes in plasmids (Stolz, 2014), which may have escaped from the metagenomic binning process (Antipov et al., 2019).

Stenotrophomonas BQ2 (MAG2) and BQ6 (MAG6) mainly harbored genes coding for final steps of metabolic pathways from monoaromatic intermediates leading to the tricarboxylic acid (TCA) cycle (*nagLK*, *ligIJK*, *galD*, *pcaF*, *xylJ*). Despite being one of the most abundant phylotypes, *Olivibacter* BQ4 (MAG4) only presented three genes related to aromatic compound degradation. It included genes encoding for one catechol 2,3-dioxygenase (*xylE*) and the final steps of the gentisate (*nagK*) and protocatechuate (*pcaF*) pathways. Accordingly, these phylotypes might be thriving on low molecular weight intermediates produced by other members of the community. In contrast, the *Pseudomonas* BQ5 genome exhibited the ability to catabolize benzoate to catechol (*xylXYZ*), and to completely assimilate catechol and protocatechuate both via *ortho*-cleavage (*catABC* and *pcaGHBCDIJF*).

Members of *Pusillimonas* (MAGs 3 and 5) and *Achromobacter* (MAGs 11 and 12) were the ones with the broadest catabolic capabilities towards aromatic substrates. These phylotypes shared almost the same predicted metabolic capabilities, being able to completely process 1-hydroxy-2-naphthoic acid, phthalate, catechol and salicylate all the way down to the central metabolism. For instance, *Pusillimonas* BQ3 (MAG3) owned the full phthalate pathway (*pht2345*), having 4 gene copies coding for phthalate 4,5-dioxygenase, and both the protocatechuate *ortho*- (*pcaGHBCDIJF*) and *meta*-cleavage pathways (*ligABC*, *galD* and *ligJK*). It also carried the entire salicylate degradation pathway via gentisate (*nagGHILK*), with 3 gene copies encoding salicylate 5-

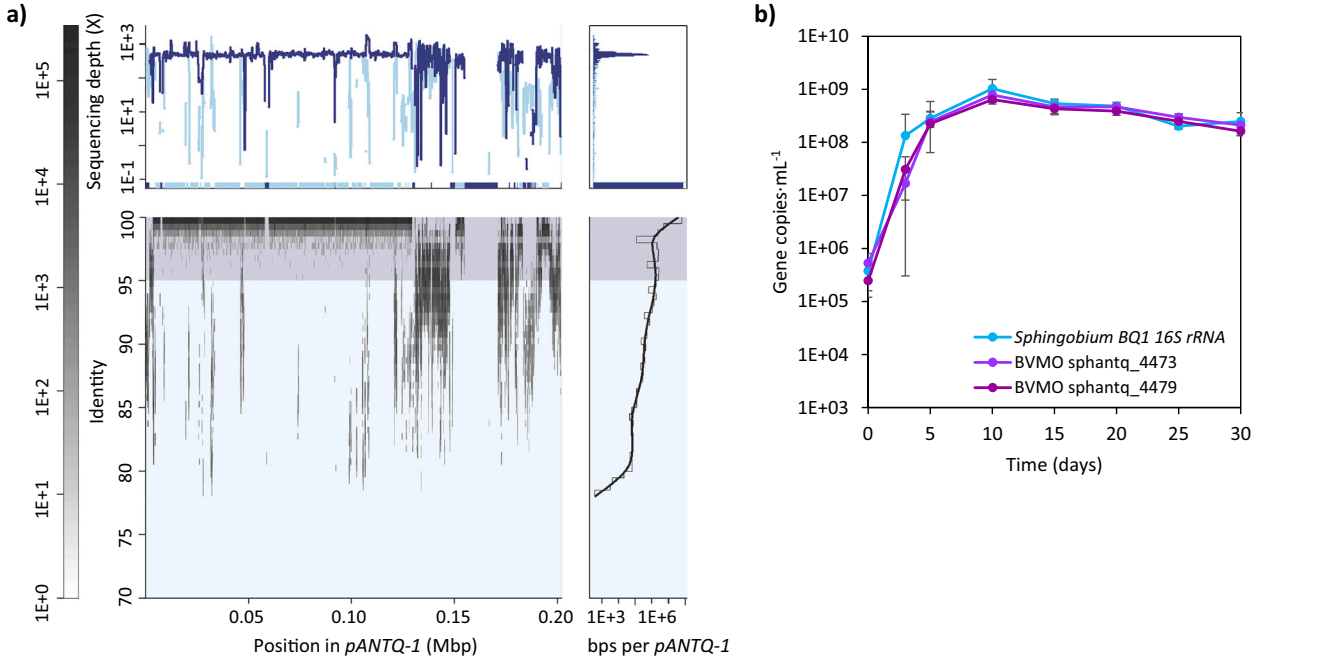

Fig. 5. (a) Recruitment plot of metagenomic reads from consortium BQ against the plasmid *pANTQ-1* from *Sphingobium* sp. AntQ-1. The sequencing depth or coverage at the top was estimated based on reads mapping at >95 % sequence identity. The plot was built using the Enveomics v.1.9.0 R package. (b) Evolution of *Sphingobium* BQ1 16S rRNA (blue) and BVMOs sphantq_4473 (light purple) and sphantq_4479 (dark purple) gene copies in sand-in-liquid cultures of consortium BQ. Values are average of three independent cultures and error bars represent standard deviation.

hydroxylase and 9 copies for gentisate 1,2-dioxygenase. This MAG also included the *nahG* gene, acting in the decarboxylation of either salicylate or 1-hydroxy-2-naphthoic acid, and genes coding for the complete cleavage of 1-hydroxy-2-naphthoic acid to phthalate (*phdIJK*). Although it did not have any genes coding for catechol 2,3-dioxygenase, it did have the rest of the genes for the *meta*-cleavage pathway (*xylEFGHIJK*). *Pusillimonas* BQ9 showed complete catabolism of catechol by both intra- and extradiol ring cleavage.

Similarly, MAGs from the *Hyphomicrobiales* order, including *Bosea* BQ11 (MAG15), *Rhizobium* (MAGs 9 and 13) and *Bradyrhizobium* BQ13 (MAG10), also displayed extensive metabolic capabilities. They all encompassed *nahG* and *xylE* genes. *Bosea* BQ11 showed the ability to completely metabolize phthalate via *ortho*-cleavage of protocatechuate (*pht2345* and *pcaGHBCDIJF*) and to catalyze the initial steps for *ortho*-cleavage of catechol (*catAB*). *Rhizobium* (MAG9) and *Bradyrhizobium* BQ13 also harbored genes for complete *ortho*-cleavage of protocatechuate. However, both *Rhizobium* MAGs generally possessed genes from intermediate steps from all pathways. In addition, *Bradyrhizobium* BQ13 was the only one of this group able to catabolize gentisate (*nagILK*).

3.6. Horizontal gene transfer of plasmid pANTQ-1

Since no unequivocal candidate BVMOs were detected in the MAGs for the initial attack of B*a*AQ, we mined for the presence of the ANTQ BVMO-hydrolase gene cluster of *Sphingobium* sp. AntQ-1, encoded on the megaplasmid *pANTQ-1* (Jiménez-Volkerink et al., 2023a), in the whole metagenomic assembly of consortium BQ. To our surprise, we not only found the BVMO gene cluster, but we also observed a 70.2 % (141,746 bp) alignment to the megaplasmid *pANTQ-1,* with just a 0.39 % mismatches and 0.018 % indels. Plasmid *pANTQ-1* carries the genes coding for the upper ANTQ degradation pathway, phthalate metabolism and catechol *meta*-cleavage pathway. The largest alignment was a 26,349 bp long fragment corresponding to positions 59,952 to 86,300 of *pANTQ-1*, which include both BVMO-hydrolase coding gene clusters and genes involved in the metabolism of catechol. Alignment to the region encoding the phthalate metabolic pathway was also observed (from positions 92,986 to 107,112; and 108,726 to 120,583). In parallel, we assessed the possible presence of strain AntQ-1 in the BQ consortium. Alignment of the primary chromosome of strain AntQ-1 only showed a 6.2 % alignment, with 2.7 % mismatches and 0.17 % indels, indicating that this strain was not a member of consortium BQ. Recruitment of metagenomic reads from consortium BQ against the plasmid *pANTQ-1* (Fig. 5a) and the primary chromosome of AntQ-1 (Fig. S5) confirmed the presence of the plasmid and the absence of strain AntQ-1 in the metagenomic library. Notably, plasmid *pANTQ-1* encompassed several genes coding for transposases and type IV secretion system components, and the corresponding genomic regions were precisely the ones that did not show significant alignment in the metagenomic assembly. Furthermore, plasmid *pANTQ-1* presented a lower GC content (60.6 %) than the average genome content (63.6 %) of *Sphingobium* sp. AntQ-1, suggesting that strain AntQ-1 already gained plasmid *pANTQ-1* from an external donor. Thus, it is likely that horizontal gene transfer events of plasmid *pANTQ-1* to a member of consortium BQ occurred in the soil microbiome.

Several studies showed that conjugative plasmid transfer from sphingomonads is basically restricted between members of the same family (Stolz, 2014). The most abundant phylotype in the consortium was *Sphingobium* BQ1, however, functional metagenomic analysis of its corresponding MAG did not reveal a clear metabolic function. Strikingly, quantification of the BVMO-coding genes sphantq_4473 and sphantq_4479 enclosed in *pANTQ-1* during active biodegradation of B*a*AQ by consortium BQ revealed identical gene copy numbers to the 16S rRNA gene from *Sphingobium* BQ1 (Fig. 5b). This is in accordance with the approximate cellular abundance of plasmid *pANTQ-1*, inferred by the plasmid read depth with respect to the chromosomal read depth in the genome of strain AntQ-1 (*chr1* 1× depth, *pANTQ-1* 0.87× depth), suggesting the presence of a single copy of *pANTQ-1* per cell. Additionally, quantification of gene transcripts also revealed a concurrent expression of the BVMO-coding genes and the 16S rRNA gene from *Sphingobium* BQ1 (Fig. S6). Altogether, our results suggest that phylotype *Sphingobium* BQ1 would be the recipient of plasmid *pANTQ-1*,

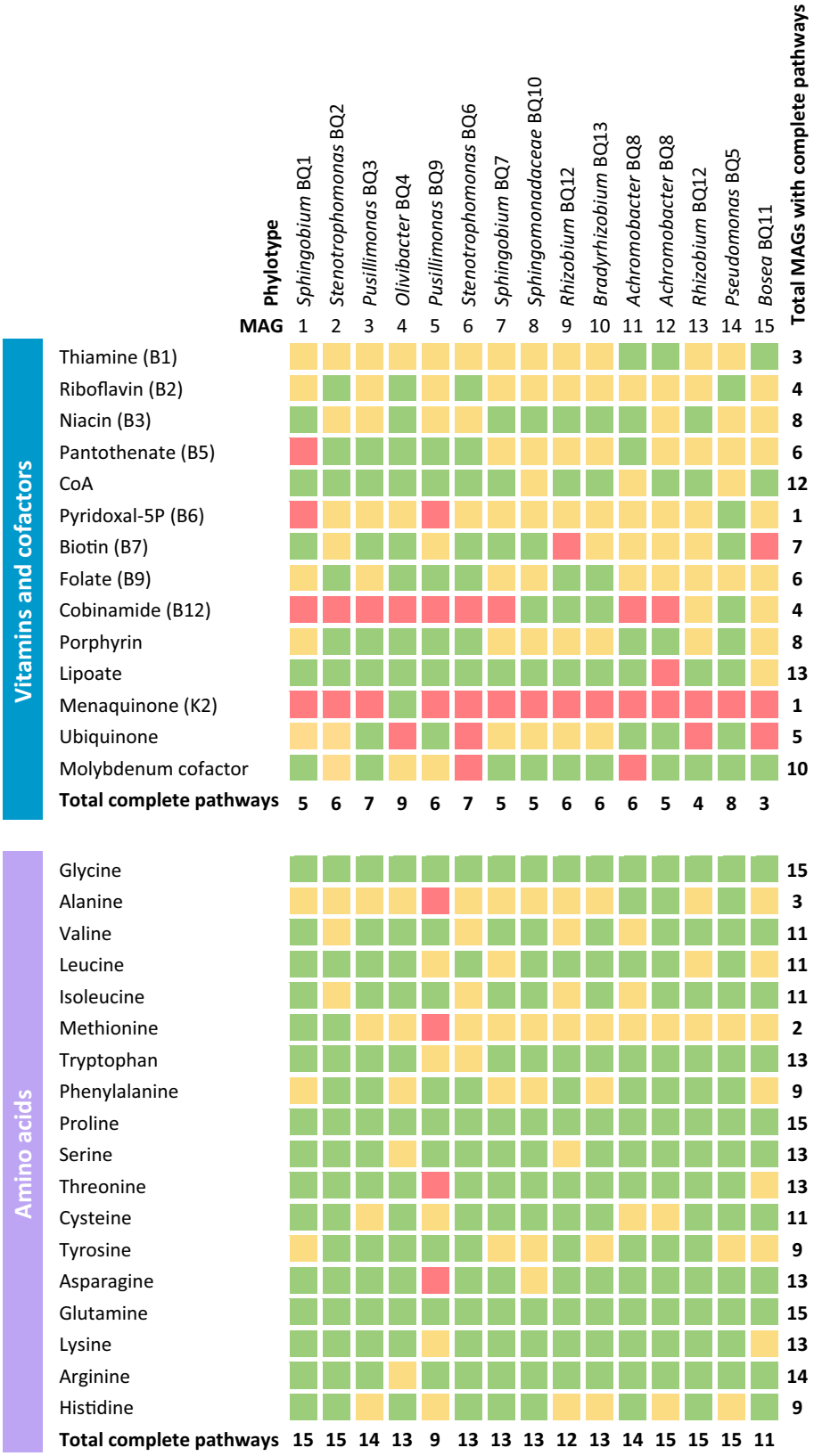

Fig. 6. Reconstruction of biosynthesis pathways of vitamins, cofactors and amino acids in the MAGs from consortium BQ. In green, complete pathway; in yellow, one or two steps missing; in red, incomplete or missing pathway. Numbers indicate the number of complete pathways for each MAG or for each cofactor, vitamin, or amino acid. Reconstruction of metabolic pathways was done using KEGG GhostKOALA.

conferring it the ability to degrade B*a*AQ. It is worth noting that the actions of the BVMOs encoded on *pANTQ-1* on B*a*AQ are consistent with the metabolomic profiles of consortium BQ and the proposed preferential degradation pathway via catechol and 1,2-naphthalenedicarboxylic acid, as these enzymes would preferentially attack the molecule from the less hindered side of the molecule, that is, next to the phenyl moiety.

3.7. Exploring the ecological roles of BQ phylotypes

Many distinct phylotypes in consortium BQ presumably had the capacity to perform the same metabolic functions, indicating functional redundancy within the microbial community (Louca et al., 2018). This seems to be a common trait of many microbial systems and it has been observed during PAH degradation in soil systems (Dunlevy et al., 2013; Guazzaroni et al., 2013). Here, functional redundancy was maintained in consortium BQ under the selective pressure of multiple transfers with B*a*AQ as the only supplied carbon source. This observation suggests that the coexisting phylotypes, despite sharing some functional traits, could have differentiated ecological roles within the community. Some key steps in the aromatic degradation pathways were only detected in a single MAG, in particular, *nahE* gene was only present in *Bradyrhizobium* BQ13 and *phdJ* was only present in *Pusillimonas* BQ3. Thus, the complete transformation of 1,2-naphthalene dicarboxylic acid, 1,2-dihydroxy-napthtalene and 1-hydroxy-2-naphthoic acid depended on the action of these particular phylotypes. This indicates the potential for syntrophic associations between the members of consortium BQ, as the rest of the community depends on specific phylotypes for further catabolism of some aromatic compounds (Morris et al., 2013). In fact, all efforts to isolate members of consortium BQ have failed, likely because of the interdependencies within partner species.

These interdependencies could also be occurring due to exchange of vitamins, amino acids and other cofactors (Seth and Taga, 2014; Zengler and Zaramela, 2018). In an attempt to decipher putative nutritional interactions in consortium BQ, we reconstructed the biosynthetic pathways of essential vitamins, cofactors and amino acids within consortium BQ MAGs (Fig. 6). None of the MAGs encompassed complete biosynthetic pathways for all the selected vitamins, cofactors and amino acids, indicating that all phylotypes were potentially auxotrophic in at least one compound. From all the pathways analyzed, MAGs presented incomplete or missing pathways for at least five compounds. Considering the large number of flavin-dependent enzymes encoded in the MAGs, including BVMOs that are key for B*a*AQ degradation, it is surprising that only *Pseudomonas* BQ5, *Olivibacter* BQ4 and *Stenotrophomonas* BQ2 and BQ6 were able to completely synthesize riboflavin (vitamin B2). Thiamine (vitamin B1), an essential cofactor for a variety of enzymes such as pyruvate dehydrogenase or pyruvate decarboxylase (Lawhorn et al., 2004), could only be predicted to be completely produced by *Bosea* BQ11 and *Achromobacter* (MAGs 11 and 12). Solely *Olivibacter* BQ4 showed the ability to synthesize menaquinone, however, this quinone is key in electron transport of anaerobic bacteria and Gram-positive bacteria, whereas aerobic Gram-negative bacteria utilize ubiquinone (Kurosu and Begari, 2010), thus, it does not seem a limiting factor in this community. Pyridoxal-5P (vitamin B6), which plays an important role in amino acid and carbohydrate metabolism (Richts et al., 2019), could only be completely produced by *Pseudomonas* BQ5. Moreover, the lack of cobinamide (vitamin B12) biosynthetic pathway was widespread among most of the consortium members, *Pseudomonas* BQ5, *Sphingomonadaceae* BQ10, *Rhizobium* BQ12 (MAG9) and *Bradyrhizobium* BQ13 were the only phylotypes with the complete pathway. Vitamin B12 is a widely required cofactor involved in the synthesis of nucleotides and amino acids, in addition to carbon processing and gene regulation, despite this, only a relatively small subset of soil bacteria is capable of its production (Lu et al., 2019). Actually, the recently described ANTQ-degrading *Sphingobium* sp. AntQ-1 is auxotrophic for this vitamin (Jiménez-Volkerink et al., 2023a).

Regarding the amino acid biosynthetic pathways, all MAGs presented incomplete pathways for at least three different amino acids. Remarkably, methionine and alanine auxotrophies were the most extended within consortium BQ, with only two and three members of the community showing complete biosynthetic pathways, respectively. Thus, it is likely that strong interdependencies occur for their supply within consortium BQ. Solely *Sphingobium* BQ1 and *Stenotrophomonas* BQ2 encoded for the complete pathway for methionine biosynthesis. Although playing an important role in the initiation of translation and in the structure of proteins, methionine is a rare and energetically costly amino acid, and many auxotrophs have been documented (Mee et al., 2014; Embree et al., 2015; Perruchon et al., 2020). Alanine, despite presenting a simple chemical structure, could only be entirely produced by *Achromobacter* (MAGs 11 and 12) and by *Pseudomonas* BQ5. *Pusillimonas* BQ9 was the only MAG lacking all the genes necessary for the biosynthesis of alanine, methionine, threonine and asparagine. Other rare amino acid biosynthetic pathways within the consortium were phenylalanine, tyrosine and histidine, which are energetically expensive amino acids. All MAGs encoded the genes for glycine, proline and glutamine, suggesting that none of the phylotypes were auxotrophic for these amino acids.

Given all the potential auxotrophies within members of consortium BQ, it seems clear that nutritional interdependencies were taking place, not only to obtain suitable carbon and energy sources from the B*a*AQ backbone, but also to supply essential nutrients and cofactors. Metabolic and nutritional cross-feeding appears to be shaping the community, where each phylotype could acquire a distinctive ecological role despite the metabolic functional redundancy.

4. Conclusions

Our results demonstrate the existence of highly specialized microbial communities in contaminated soils responsible for processing oxy-PAHs. The combination of metabolomic and metagenomic functional gene analyses of the B*a*AQ-degrading consortium revealed that the B*a*AQ metabolic pathway was initiated by BVMOs encoded in plasmid *pANTQ-1*. BV oxidations could be a relevant mechanism for the processing of oxy-PAHs in contaminated sites, thus contributing to mitigate the potential risk of their accumulation during bioremediation. Therefore, biostimulation strategies should guarantee not only enhancement of PAH-degraders activity but also that of the oxy-PAH-degrading specialists. Biomarkers based on the detection of BVMO genes could be a valuable molecular proxy to assess this activity. The genome wide metagenomic functional analysis provided a valuable insight into the interactions within this soil microbial consortium, identifying the interdependencies that shape the microbial community and assemble a stable and efficient B*a*AQ degrading microbial network.

CRediT authorship contribution statement

Sara N. Jiménez-Volkerink: Conceptualization, Formal analysis, Investigation, Writing – original draft, Visualization. **Maria Jordán:** Investigation, Formal analysis. **Hauke Smidt:** Resources, Writing – review & editing, Supervision, Funding acquisition. **Cristina Minguillón:** Writing – review & editing. **Joaquim Vila:** Conceptualization, Resources, Writing – review & editing, Supervision, Project administration, Funding acquisition. **Magdalena Grifoll:** Conceptualization, Resources, Writing – review & editing, Supervision, Project administration, Funding acquisition.

Declaration of competing interest

The authors declare that they have no known competing financial interests or personal relationships that could have appeared to influence the work reported in this paper.

Data availability

All sequencing data are available in open repositories

Acknowledgements

This work received funding from the Ministry of Science and Innovation, Spain, grant number PID2019-109700RB-C22. SNJV was supported by an FPU fellowship (grant number FPU15/06077) of the Ministry of Education, Culture and Sports, Spain. MJ is supported by an FPI fellowship (grant number PRE2020-093013) funded by the Ministry of Science and Innovation, Spain. JV is a Serra Húnter Professor (Generalitat de Catalunya). Funding from the Dutch Research Council, The Netherlands to HS through the UNLOCK project (NRGWI.obrug.2018.005) is acknowledged. SNJV, MJ, JV and MG are members of the Water Research Institute from the University of Barcelona (IdRA-UB). We would like to thank Sudarshan Shetty for his help with metagenome assembly and discussions.

Appendix A. Supplementary data

Supplementary data to this article can be found online at https://doi.org/10.1016/j.scitotenv.2023.167832.

References

Adrion, A.C., Singleton, D.R., Nakamura, J., Shea, D., Aitken, M.D., 2016. Improving polycyclic aromatic hydrocarbon biodegradation in contaminated soil through low-level surfactant addition after conventional bioremediation. Environ. Eng. Sci. 33 (9), 659–670. https://doi.org/10.1089/ees.2016.0128.

Andersson, B.E., Lundstedt, S., Tornberg, K., Schnürer, Y., Öberg, L.G., Mattiasson, B., 2003. Incomplete degradation of polycyclic aromatic hydrocarbons in soil inoculated with wood-rotting fungi and their effect on the indigenous soil bacteria. Environ. Toxicol. Chem. 22 (6), 1238–1243. https://doi.org/10.1002/etc.5620220608.

Antipov, D., Raiko, M., Lapidus, A., Pevzner, P.A., 2019. Plasmid detection and assembly in genomic and metagenomic data sets. Genome Res. 29 (6), 961–968. https://doi.org/10.1101/GR.241299.118.

Aylward, F.O., McDonald, B.R., Adams, S.M., Valenzuela, A., Schmidt, R.A., Goodwin, L. A., Woyke, T., Currie, C.R., Suen, G., Poulsen, M., 2013. Comparison of 26 sphingomonad genomes reveals diverse environmental adaptations and biodegradative capabilities. Appl. Environ. Microbiol. 79 (12), 3724–3733. https://doi.org/10.1128/AEM.00518-13.

Balashova, N.V., Stolz, A., Knackmuss, H.J., Kosheleva, I.A., Naumov, A.V., Boronin, A. M., 2001. Purification and characterization of a salicylate hydroxylase involved in 1-hydroxy-2-naphthoic acid hydroxylation from the naphthalene and phenanthrene-degrading bacterial strain Pseudomonas putida BS202-P1. Biodegradation 12 (3), 179–188. https://doi.org/10.1023/A:1013126723719/METRICS.

Belda, E., Heck, R.G.A. van, Lopez-Sanchez, M.J., Cruveiller, S., Barbe, V., Fraser, C., Klenk, H.-P., Petersen, J., Morgat, A., Nikel, P.I., Vallenet, D., Rouy, Z., Sekowska, A., Santos, V.A.P.M. dos, Lorenzo, V. de, Danchin, A., Médigue, C., 2016. The revisited genome of Pseudomonas putida KT2440 enlightens its value as a robust metabolic chassis. Environ. Microbiol. 18 (10), 3403–3424. https://doi.org/10.1111/1462-2920.13230.

Cajthaml, T., Erbanová, P., Šašek, V., Moeder, M., 2006. Breakdown products on metabolic pathway of degradation of benz[a]anthracene by a ligninolytic fungus. Chemosphere 64 (4), 560–564. https://doi.org/10.1016/j.chemosphere.2005.11.034.

Chaumeil, P.A., Mussig, A.J., Hugenholtz, P., Parks, D.H., 2020. GTDB-Tk: a toolkit to classify genomes with the genome taxonomy database. Bioinformatics 36 (6), 1925–1927. https://doi.org/10.1093/BIOINFORMATICS/BTZ848.

Chibwe, L., Geier, M.C., Nakamura, J., Tanguay, R.L., Aitken, M.D., Simonich, S.L.M., 2015. Aerobic bioremediation of PAH contaminated soil results in increased genotoxicity and developmental toxicity. Environ. Sci. Tech. 49 (23), 13889–13898. https://doi.org/10.1021/acs.est.5b00499.

Clergé, A., Le Goff, J., Lopez, C., Ledauphin, J., Delépée, R., 2019. Oxy-PAHs: occurrence in the environment and potential genotoxic/mutagenic risk assessment for human health. Crit. Rev. Toxicol. 49 (4), 302–328. https://doi.org/10.1080/10408444.2019.1605333.

Cole, J.R., Wang, Q., Fish, J.A., Chai, B., McGarrell, D.M., Sun, Y., Brown, C.T., Porras-Alfaro, A., Kuske, C.R., Tiedje, J.M., 2014. Ribosomal database project: data and tools for high throughput rRNA analysis. Nucleic Acids Res. 42 (Database issue), D633. https://doi.org/10.1093/NAR/GKT1244.

Corteselli, E.M., Aitken, M.D., Singleton, D.R., 2017. Description of Immundisolibacter cernigliae gen. Nov., sp. nov., a high-molecular-weight polycyclic aromatic hydrocarbondegrading bacterium within the class Gammaproteobacteria, and proposal of Immundisolibacterales Ord. Nov. and Immundisolibacteraceae fa. Int. J. Syst. Evol. Microbiol. 67 (4), 925–931. https://doi.org/10.1099/ijsem.0.001714.

Dasgupta, S., Cao, A., Mauer, B., Yan, B., Uno, S., McElroy, A., 2014. Genotoxicity of oxy-PAHs to Japanese medaka (Oryzias latipes) embryos assessed using the comet assay. Environ. Sci. Pollut. Res. 21 (24), 13867–13876. https://doi.org/10.1007/s11356-014-2586-4.

Deka, H., Lahkar, J., 2017. Biodegradation of benzo(a)anthracene employing Paenibacillus sp. HD1PAH: a novel strain isolated from crude oil contaminated soil. Polycycl. Aromat. Compd. 37 (2–3), 161–169. https://doi.org/10.1080/10406638.2016.1253593.

Dunlevy, S.R., Singleton, D.R., Aitken, M.D., 2013. Biostimulation reveals functional redundancy of anthracene-degrading bacteria in polycyclic aromatic hydrocarbon-contaminated soil. Environ. Eng. Sci. 30 (11), 697–705. https://doi.org/10.1089/ees.2013.0067.

Embree, M., Liu, J.K., Al-Bassam, M.M., Zengler, K., 2015. Networks of energetic and metabolic interactions define dynamics in microbial communities. Proc. Natl. Acad. Sci. U. S. A. 112 (50), 15450–15455. https://doi.org/10.1073/PNAS.1506034112/-/DCSUPPLEMENTAL/PNAS.1506034112.SD03.XLSX.

Fraaije, M.W., Kamerbeek, N.M., Van Berkel, W.J.H., Janssen, D.B., 2002. Identification of a Baeyer-Villiger monooxygenase sequence motif. FEBS Lett. 518 (1–3), 43–47. https://doi.org/10.1016/S0014-5793(02)02623-6.

Grifoll, M., Casellas, M., Bayona, J.M., Solanas, A.M., 1992. Isolation and characterization of a fluorene-degrading bacterium: identification of ring oxidation and ring fission products. Appl. Environ. Microbiol. 58 (9), 2910–2917. https://doi.org/10.1128/aem.58.9.2910-2917.1992.

Guazzaroni, M.-E., Herbst, F.-A., Lores, I., Tamames, J., Peláez, A.I., López-Cortés, N., Alcaide, M., Del Pozo, M.V., Vieites, J.M., von Bergen, M., Gallego, J.L.R., Bargiela, R., López-López, A., Pieper, D.H., Rosselló-Móra, R., Sánchez, J., Seifert, J., Ferrer, M., 2013. Metaproteogenomic insights beyond bacterial response to naphthalene exposure and bio-stimulation. ISME J. 7 (1), 122–136. https://doi.org/10.1038/ismej.2012.82.

Hareland, W.A., Crawford, R.L., Chapman, P.J., Dagley, S., 1975. Metabolic function and properties of 4-hydroxyphenylacetic acid 1-hydroxylase from Pseudomonas acidovorans. J. Bacteriol. 121 (1), 272–285. https://doi.org/10.1128/jb.121.1.272-285.1975.

Hu, J., Adrion, A.C., Nakamura, J., Shea, D., Aitken, M.D., 2014. Bioavailability of (geno) toxic contaminants in polycyclic aromatic hydrocarbon-contaminated soil before and after biological treatment. Environ. Eng. Sci. 31 (4), 176–182. https://doi.org/10.1089/ees.2013.0409.

Idowu, O., Semple, K.T., Ramadass, K., O'Connor, W., Hansbro, P., Thavamani, P., 2019. Beyond the obvious: environmental health implications of polar polycyclic aromatic hydrocarbons. Environ. Int. 123 (December 2018), 543–557. https://doi.org/10.1016/j.envint.2018.12.051.

Iwaki, H., Grosse, S., Bergeron, H., Leisch, H., Morley, K., Hasegawa, Y., Lau, P.C.K., 2013. Camphor pathway redux: functional recombinant expression of 2,5-and 3,6-diketocamphane monooxygenases of Pseudomonas putida ATCC 17453 with their cognate flavin reductase catalyzing Baeyer-Villiger reactions. Appl. Environ. Microbiol. 79 (10), 3282–3293. https://doi.org/10.1128/AEM.03958-12.

Jiménez-Volkerink, S.N., Vila, J., Jordán, M., Minguillón, C., Smidt, H., Grifoll, M., 2023a. Multi-Omic profiling of a newly isolated oxy-PAH degrading specialist from PAH-contaminated soil reveals bacterial mechanisms to mitigate the risk posed by polar transformation products. Environ. Sci. Technol. 57 (1), 139–149. https://doi.org/10.1021/acs.est.2c05485.

Jiménez-Volkerink, S.N., Jordán, M., Singleton, D.R., Grifoll, M., Vila, J., 2023b. Bacterial benz(a)anthracene catabolic networks in contaminated soils and their modulation by other co-occurring HMW-PAHs. Environ. Pollut. 328, 121624 https://doi.org/10.1016/j.envpol.2023.121624.

Jones, M.D., Singleton, D.R., Sun, W., Aitken, M.D., 2011. Multiple DNA extractions coupled with stable-isotope probing of anthracene-degrading Bacteria in contaminated soil. Appl. Environ. Microbiol. 77 (9), 2984–2991. https://doi.org/10.1128/AEM.01942-10.

Kanaly, R.A., Harayama, S., 2010. Advances in the field of high-molecular-weight polycyclic aromatic hydrocarbon biodegradation by bacteriambt-130 136..164. J. Microbial. Biotechnol. 3 (2), 136–164. https://doi.org/10.1111/j.1751-7915.2009.00130.x.

Kozich, J.J., Westcott, S.L., Baxter, N.T., Highlander, S.K., Schloss, P.D., 2013. Development of a dual-index sequencing strategy and curation pipeline for analyzing amplicon sequence data on the miseq illumina sequencing platform. Appl. Environ. Microbiol. 79 (17), 5112–5120. https://doi.org/10.1128/AEM.01043-13.

Kurosu, M., Begari, E., 2010. Vitamin K2 in Electron transport system: are enzymes involved in vitamin K2 biosynthesis promising drug targets? Molecules 15 (3), 1531. https://doi.org/10.3390/MOLECULES15031531.

Langmead, B., Salzberg, S.L., 2012. Fast gapped-read alignment with bowtie 2. Nat. Methods 9 (4), 357–359. https://doi.org/10.1038/NMETH.1923, 2012 9:4.

Larsson, M., Lam, M.M., Van Hees, P., Giesy, J.P., Engwall, M., 2018. Occurrence and leachability of polycyclic aromatic compounds in contaminated soils: chemical and bioanalytical characterization. Sci. Total Environ. 622–623, 1476–1484. https://doi.org/10.1016/j.scitotenv.2017.12.015.

Lawhorn, B.G., Mehl, R.A., Begley, T.P., 2004. Biosynthesis of the thiamin pyrimidine: the reconstitution of a remarkable rearrangement reaction. Org. Biomol. Chem. 2 (17), 2538–2546. https://doi.org/10.1039/B405429F.

Lee, B.D., Hosomi, M., 2001. A hybrid fenton oxidation-microbial treatment for soil highly contaminated with benz(a)anthracene. Chemosphere 43 (8), 1127–1132. https://doi.org/10.1016/s0045-6535(00)00182-x.

Lehto, K.M., Puhakka, J.A., Lemmetyinen, H., 2003. Biodegradation of selected UV-irradiated and non-irradiated polycyclic aromatic hydrocarbons (PAHs). Biodegradation 14 (4), 249–263. https://doi.org/10.1023/a:1024704505832.

Li, X., Pan, Y., Hu, S., Cheng, Y., Wang, Y., Wu, K., Zhang, S., Yang, S., 2018. Diversity of phenanthrene and benz[a]anthracene metabolic pathways in white rot fungus Pycnoporus sanguineus 14. Int. Biodeterior. Biodegrad. 134, 25–30. https://doi.org/10.1016/j.ibiod.2018.07.012.

Louca, S., Polz, M.F., Mazel, F., Albright, M.B.N., Huber, J.A., O'Connor, M.I., Ackermann, M., Hahn, A.S., Srivastava, D.S., Crowe, S.A., Doebeli, M., Parfrey, L.W., 2018. Function and functional redundancy in microbial systems. Nat. Ecol. Evol. 2 (6), 936–943. https://doi.org/10.1038/s41559-018-0519-1.

Lu, X., Heal, K.R., Ingalls, A.E., Doxey, A.C., Neufeld, J.D., 2019. Metagenomic and chemical characterization of soil cobalamin production. ISME J. 14 (1), 53–66. https://doi.org/10.1038/s41396-019-0502-0, 2019 14:1.

Lundstedt, S., Haglund, P., Öberg, L., 2003. Degradation and formation of polycyclic aromatic compounds during bioslurry treatment of an aged gasworks soil. Environ. Toxicol. Chem. 22 (7), 1413–1420. https://doi.org/10.1002/etc.5620220701.

Lundstedt, S., White, P.A., Lemieux, C.L., Lynes, K.D., Lambert, I.B., Öberg, L., Haglund, P., Tysklind, M., 2007. Sources, fate, and toxic hazards of oxygenated polycyclic aromatic hydrocarbons (PAHs) at PAH-contaminated sites. Ambio 36 (6), 475–485. https://doi.org/10.1579/0044-7447(2007)36[475:SFATHO]2.0.CO;2.

Luo, A., Wu, Y.R., Xu, Y., Kan, J., Qiao, J., Liang, L., Huang, T., Hu, Z., 2016. Characterization of a cytochrome P450 monooxygenase capable of high molecular weight PAHs oxidization from Rhodococcus sp. P14. Process Biochem. 51 (12), 2127–2133. https://doi.org/10.1016/J.PROCBIO.2016.07.024.

Maidak, B.L., Cole, J.R., Lilburn, T.G., Parker, C.T., Saxman, P.R., Farris, R.J., Garrity, G. M., Olsen, G.J., Schmidt, T.M., Tiedje, J.M., 2001. The RDP-II (ribosomal database project). Nucleic Acids Res. 29 (1), 173–174. https://doi.org/10.1093/nar/29.1.173.

Mallick, S., Chakraborty, J., Dutta, T.K., 2011. Role of oxygenases in guiding diverse metabolic pathways in the bacterial degradation of low-molecular-weight polycyclic aromatic hydrocarbons: a review. Crit. Rev. Microbiol. 37 (1), 64–90. https://doi.org/10.3109/1040841X.2010.512268.

McCarrick, S., Cunha, V., Zapletal, O., Vondráček, J., Dreij, K., 2019. In vitro and in vivo genotoxicity of oxygenated polycyclic aromatic hydrocarbons. Environ. Pollut. 246, 678–687. https://doi.org/10.1016/j.envpol.2018.12.092.

Mee, M.T., Collins, J.J., Church, G.M., Wang, H.H., 2014. Syntrophic exchange in synthetic microbial communities. Proc. Natl. Acad. Sci. U. S. A. 111 (20), E2149. https://doi.org/10.1073/PNAS.1405641111.

Moody, J.D., Freeman, J.P., Doerge, D.R., Cerniglia, C.E., 2001. Degradation of Phenanthrene and anthracene by cell suspensions of Mycobacterium sp. strain PYR-1. Appl. Environ. Microbiol. 67 (4), 1476–1483. https://doi.org/10.1128/AEM.67.4.1476-1483.2001.

Moody, J.D., Freeman, J.P., Cerniglia, C.E., 2005. Degradation of benz[a]anthracene by Mycobacterium vanbaalenii strain PYR-1. Biodegradation 16 (6), 513–526. https://doi.org/10.1007/s10532-004-7217-1.

Morris, B.E.L., Henneberger, R., Huber, H., Moissl-Eichinger, C., 2013. Microbial syntrophy: interaction for the common good. FEMS Microbiol. Rev. 37 (3), 384–406. https://doi.org/10.1111/1574-6976.12019.

Muyzer, G., De Waal, E.C., Uitterlinden, A.G., 1993. Profiling of complex microbial populations by denaturing gradient gel electrophoresis analysis of polymerase chain reaction-amplified genes coding for 16S rRNA. Appl. Environ. Microbiol. 59 (3), 695–700. https://doi.org/10.1128/aem.59.3.695-700.1993.

Nurk, S., Meleshko, D., Korobeynikov, A., Pevzner, P.A., 2017. MetaSPAdes: a new versatile metagenomic assembler. Genome Res. 27 (5), 824–834. https://doi.org/10.1101/GR.213959.116/-/DC1.

Oksanen, J., Blanchet, F.G., Friendly, M., Kindt, R., Legendre, P., Mcglinn, D., Minchin, P. R., O'hara, R.B., Simpson, G.L., Solymos, P., Henry, M., Stevens, H., Szoecs, E., Maintainer, H.W., 2020. Package "vegan": community ecology package version 2.5-7. In *cran.ism.ac.jp*. http://cran.ism.ac.jp/web/packages/vegan/vegan.pdf.

Parks, D.H., Imelfort, M., Skennerton, C.T., Hugenholtz, P., Tyson, G.W., 2015. CheckM: assessing the quality of microbial genomes recovered from isolates, single cells, and metagenomes. Genome Res. 25 (7), 1043. https://doi.org/10.1101/GR.186072.114.

Perruchon, C., Vasileiadis, S., Papadopoulou, E.S., Karpouzas, D.G., 2020. Genome-based metabolic reconstruction unravels the key role of B12 in methionine Auxotrophy of an Ortho-Phenylphenol-degrading Sphingomonas haloaromaticamans. Front. Microbiol. 10, 3009. https://doi.org/10.3389/FMICB.2019.03009/BIBTEX.

Quast, C., Pruesse, E., Yilmaz, P., Gerken, J., Schweer, T., Yarza, P., Peplies, J., Glöckner, F.O., 2013. The SILVA ribosomal RNA gene database project: improved data processing and web-based tools. Nucleic Acids Res. 41 (D1), D590–D596. https://doi.org/10.1093/NAR/GKS1219.

Richts, B., Rosenberg, J., Commichau, F.M., 2019. A survey of pyridoxal 5′-phosphate-dependent proteins in the gram-positive model bacterium Bacillus subtilis. Front. Mol. Biosci. 6 (MAY), 32. https://doi.org/10.3389/FMOLB.2019.00032.

Rodgers-Vieira, E.A., Zhang, Z., Adrion, A.C., Gold, A., Aitken, M.D., 2015. Identification of Anthraquinone-degrading bacteria in soil contaminated with polycyclic aromatic hydrocarbons. Appl. Environ. Microbiol. 81 (11), 3775–3781. https://doi.org/10.1128/AEM.00033-15.

Seemann, T., 2014. Prokka: rapid prokaryotic genome annotation. Bioinformatics (Oxf. Engl.) 30 (14), 2068–2069. https://doi.org/10.1093/BIOINFORMATICS/BTU153.

Seo, J.S., Keum, Y.S., Hu, Y., Lee, S.E., Li, Q.X., 2006. Phenanthrene degradation in Arthrobacter sp. P1-1: initial 1,2-, 3,4- and 9,10-dioxygenation, and meta- and ortho-cleavages of naphthalene-1,2-diol after its formation from naphthalene-1,2-dicarboxylic acid and hydroxyl naphthoic acids. Chemosphere 65 (11), 2388–2394. https://doi.org/10.1016/j.chemosphere.2006.04.067.

Seth, E.C., Taga, M.E., 2014. Nutrient cross-feeding in the microbial world. Front. Microbiol. 0 (JULY), 350. https://doi.org/10.3389/FMICB.2014.00350.

Stolz, A., 2014. Degradative plasmids from sphingomonads. FEMS Microbiol. Lett. 350 (1), 9–19. https://doi.org/10.1111/1574-6968.12283.

Tauler, M., Vila, J., Nieto, J.M., Grifoll, M., 2016. Key high molecular weight PAH-degrading bacteria in a soil consortium enriched using a sand-in-liquid microcosm system. Appl. Microbiol. Biotechnol. 100 (7), 3321–3336. https://doi.org/10.1007/s00253-015-7195-8.

Tian, Z., Gold, A., Nakamura, J., Zhang, Z., Vila, J., Singleton, D.R., Collins, L.B., Aitken, M.D., 2017. Nontarget analysis reveals a bacterial metabolite of pyrene implicated in the genotoxicity of contaminated soil after bioremediation. Environ. Sci. Technol. 51 (12), 7091–7100. https://doi.org/10.1021/acs.est.7b01172.

Tolmie, C., Smit, M.S., Opperman, D.J., 2019. Native roles of Baeyer-Villiger monooxygenases in the microbial metabolism of natural compounds. In: Natural Product Reports, Vol. 36, Issue 2. Royal Society of Chemistry, pp. 326–353. https://doi.org/10.1039/c8np00054a.

van Berkel, W.J.H., Kamerbeek, N.M., Fraaije, M.W., 2006. Flavoprotein monooxygenases, a diverse class of oxidative biocatalysts. J. Biotechnol. 124 (4), 670–689. https://doi.org/10.1016/j.jbiotec.2006.03.044.

van Herwijnen, R., Wattiau, P., Bastiaens, L., Daal, L., Jonker, L., Springael, D., Govers, H.A.J., Parsons, J.R., 2003. Elucidation of the metabolic pathway of fluorene and cometabolic pathways of phenanthrene, fluoranthene, anthracene and dibenzothiophene by *Sphingomonas* sp. LB126. Res. Microbiol. 154, 199–206. https://doi.org/10.1016/S0923-2508(03)00039-1.

Weisburg, W.G., Barns, S.M., Pelletier, D.A., Lane, D.J., 1991. 16S ribosomal DNA amplification for phylogenetic study. J. Bacteriol. 173 (2), 697–703. https://doi.org/10.1128/jb.173.2.697-703.1991.

Wilcke, W., Kiesewetter, M., Musa Bandowe, B.A., 2014. Microbial formation and degradation of oxygen-containing polycyclic aromatic hydrocarbons (OPAHs) in soil during short-term incubation. Environ. Pollut. 184, 385–390. https://doi.org/10.1016/j.envpol.2013.09.020.

Wu, Y.-R., Luo, Z.-H., Vrijmoed, L.L.P., 2010. Biodegradation of anthracene and benz[a] anthracene by two fusarium solani strains isolated from mangrove sediments. Bioresour. Technol. 101 (24), 9666–9672. https://doi.org/10.1016/j.biortech.2010.07.049.

Yao, J.J., Huang, Z.H., Masten, S.J., 1998. The ozonation of benz[a]anthracene: pathway and product identification. Water Res. 32 (11), 3235–3244. https://doi.org/10.1016/S0043-1354(98)00094-3.

Zengler, K., Zaramela, L.S., 2018. The social network of microorganisms — how auxotrophies shape complex communities. Nat. Rev. Microbiol. 16 (6), 383–390. https://doi.org/10.1038/S41579-018-0004-5, 2018 16:6.